Brain, Behavior, and Immunity 59 (2017) 103–117

Contents lists available at ScienceDirect

Brain, Behavior, and Immunity

journal homepage: www.elsevier.com/locate/ybrbi

Full-length Article

The quality of cortical network function recovery depends on localization and degree of axonal demyelination

Manuela Cerina [a,*,1], Venu Narayanan [a,1], Kerstin Göbel [a], Stefan Bittner [b], Tobias Ruck [a], Patrick Meuth [a], Alexander M. Herrmann [a], Martin Stangel [c], Viktoria Gudi [d], Thomas Skripuletz [d], Thiemo Daldrup [e], Heinz Wiendl [a], Thomas Seidenbecher [e], Petra Ehling [a], Christoph Kleinschnitz [f], Hans-Christian Pape [e,1], Thomas Budde [e,1], Sven G. Meuth [a,*,1]

[a] Department of Neurology, University of Münster, Münster, Germany
[b] Department of Neurology, University Medical Center of the Johannes Gutenberg-University Mainz, Mainz, Germany
[c] Clinical Neuroimmunology and Neurochemistry, Department of Neurology, Hannover Medical School and Centre for Systems Neuroscience, Hannover, Germany
[d] Department of Neurology, Hannover Medical School, Hannover, Germany
[e] Institute of Physiology I, University of Münster, Münster, Germany
[f] Department of Neurology, University of Würzburg, Würzburg, Germany

ARTICLE INFO

Article history:
Received 12 March 2016
Received in revised form 12 August 2016
Accepted 25 August 2016
Available online 25 August 2016

Keywords:
Demyelination
Remyelination
Thalamocortical system
White matter lesion
Gray matter lesion

ABSTRACT

Myelin loss is a severe pathological hallmark common to a number of neurodegenerative diseases, including multiple sclerosis (MS). Demyelination in the central nervous system appears in the form of lesions affecting both white and gray matter structures. The functional consequences of demyelination on neuronal network and brain function are not well understood. Current therapeutic strategies for ameliorating the course of such diseases usually focus on promoting remyelination, but the effectiveness of these approaches strongly depends on the timing in relation to the disease state. In this study, we sought to characterize the time course of sensory and behavioral alterations induced by de- and remyelination to establish a rational for the use of remyelination strategies. By taking advantage of animal models of general and focal demyelination, we tested the consequences of myelin loss on the functionality of the auditory thalamocortical system: a well-studied neuronal network consisting of both white and gray matter regions. We found that general demyelination was associated with a permanent loss of the tonotopic cortical organization *in vivo*, and the inability to induce tone-frequency-dependent conditioned behaviors, a status persisting after remyelination. Targeted, focal lysolecithin-induced lesions in the white matter fiber tract, but not in the gray matter regions of cortex, were fully reversible at the morphological, functional and behavioral level. These findings indicate that remyelination of white and gray matter lesions have a different functional regeneration potential, with the white matter being able to regain full functionality while cortical gray matter lesions suffer from permanently altered network function. Therefore therapeutic interventions aiming for remyelination have to consider both region- and time-dependent strategies.

1. Introduction

Processes influencing axonal myelination, including myelin loss and gain, are well known physiological events. Severe pathophysiological alterations of the degree of myelination are peculiar hallmarks of a number of neurodegenerative diseases, including multiple sclerosis (MS; Meuth et al., 2010). In MS patients, intermingled episodes of de- and remyelination are associated with the occurrence of gray and white matter lesions in brain and spinal cord. Furthermore, converging evidence relates the occurrence of lesions to the onset or worsening of disease symptoms (Franklin et al., 2012). Myelin plays multiple physiological roles and it is intuitive that its loss may have severe consequences; after all, myelin integrity is important for neuronal and axonal survival, as well as faithful transmission of information in a given network of the central nervous system (CNS; Yates, 2014; Nave and Werner, 2014). In line with white matter damage, MS patients often are

* Corresponding authors at: University of Münster, Department of Neurology, Albert-Schweitzer-Campus 1, Building A1, 48149 Münster, Germany.
E-mail addresses: manuela.cerina@ukmuenster.de (M. Cerina), sven.meuth@ukmuenster.de (S.G. Meuth).
[1] Equal contributions by first (MC, VN) and senior authors (HCP, TB and SGM).

http://dx.doi.org/10.1016/j.bbi.2016.08.014
0889-1591/

diagnosed with altered conduction latencies in the CNS (Kim et al., 2013) as indicated by delayed evoked auditory, sensory, motor and visual potentials (Markianos et al., 2009; Matas et al., 2010; Niklas et al., 2009).

Physicians and researchers are now developing new therapeutic strategies to ameliorate disease symptoms by promoting remyelination. This attempt is fueled by recent evidence demonstrating that myelin is required for learning motor tasks and similarly how the acquisition of new information promotes myelin synthesis, both in humans and rodents (Franklin and Gallo, 2014; McKenzie et al., 2014). Indeed, this approach has already been adopted in many clinical trials, but positive results have not been observed in all patients (Bhatt et al., 2014). Therefore strategies to identify eligible patients with highest possible benefit are urgently needed. In this context, it is important to note that numerous MS patients also report severe learning and cognitive dysfunctions in addition to locomotor impairment (Hulst et al., 2013; Manrique-Hoyos et al., 2012), and none of these symptoms can be fully explained by massive or local myelin loss alone. New techniques used for MS diagnosis point to many gray matter structures being severely damaged in MS patients (Hulst and Geurts, 2011). In particular, the thalamocortical system seems to be susceptible as cortical atrophy (Deppe et al., 2014; Minagar et al., 2013) and thalamic lesions as well as lesion-independent degeneration are often observed very early in the disease course. In the light of such evidence and the obvious complexity of MS pathophysiology, the aim of our study was to investigate functional consequences of various demyelination strategies and then to allow endogenous remyelination. By taking into consideration the diversity (whether white or gray matter) and the timing of the lesions we tried to establish a rational for optimal remyelinating intervention times. In this way we tried to answer the following questions: (i) Is promoting remyelination a beneficial strategy? And, if so, (ii) does the success of promoting remyelination depend on the localization of the lesion? (iii) Does the time of intervention/remyelination affect the course of the disease?

In order to answer these questions, we needed to isolate the demyelinating events from other MS hallmarks, an attempt which was possible only by performing a translational study in animal models. We choose to use (i) the cuprizone model of general de- and remyelination to determine the consequences of massive myelin loss and re-growth and (ii) the lysolecithin model of focal demyelination which allowed us to target locally restricted white or gray matter lesions. We combined electrophysiology *in vivo* with behavioral assays in freely behaving animals to investigate the thalamocortical system which, besides being the "hot spot" for gray matter lesions occurring in MS patients, has the advantage of being a highly interconnected network featuring an extensive white fiber tract (the internal capsule).

2. Materials and methods

2.1. Animals and experimental design

All animal work was performed in accordance with the 2010/63/EU of the European Parliament and of the Council of 22 September 2010 and has been approved by the local authorities (Landesamt für Natur, Umwelt und Verbraucherschutz Nordrhein-Westfalen; approval ID: 87-51.04.2010.A331). All efforts were made to minimize the number of animals used and to avoid their stress and suffering strictly following the ARRIVE guidelines (Kilkenny et al., 2010). C57BL6 mice were used for all the experiments and were singly caged, kept in a 12-h light/dark cycle, and food and water were available *ad libitum*.

2.1.1. Cuprizone treatment

C57BL6 mice were used for all experiments. The animals were 2–3 months old at the beginning of the experiments. Experimental toxic demyelination was induced by feeding mice a diet containing 0.2% cuprizone (bis-cyclohexanone oxaldihydrazone, Sigma-Aldrich Inc., Hamburg, Germany) mixed into a ground standard rodent chow (Skripuletz et al., 2011). The cuprizone diet was maintained for 5–6 weeks. A second group, matched for age and sex, served as control. Interruption of cuprizone administration favors spontaneous remyelination (Skripuletz et al., 2008), therefore we tested two other groups, 7 and 25 days after re-introduction of normal food (7-day remyelination and 25-day remyelination in the text). In order to assess long term effects, an additional group of animals was tested 45 days after stopping the treatment.

2.1.2. Lysolecithin injections

Anesthesia was induced with isoflurane (3% in O_2; Abbot GmbH & Co. KG, Wiesbaden, Germany), maintained with i.p. injection of pentobarbital (50 mg/kg, Narcoren, Merial GmbH, Germany), and additional doses were given if necessary (10–15% of the initial dose). All pressure points were covered with 2% xylocaine gel (Astra Zeneca GmbH, Wedel, Germany) and tissue to be incised was injected with 2% xylocaine solution. Corneas were protected with a dexpanthenol-containing gel (Bepanthen®, Bayer, Leverkusen, Germany). When animals were already anesthetized, before beginning with the surgery, they received an additional injection of carprofen (Rymadil, 5 mg/kg) in order to relieve post-operatory pain. The head was mounted in a stereotaxic apparatus (ASI Instruments, Inc., Warren, MI, USA) via ear bars, and the levels of bregma and lambda were equalized. Craniotomies were performed unilaterally (left hemisphere), thus one hemisphere served as control. The dura mater was removed and then, by means of a Hamilton syringe, lysolecithin (2 µl; at a speed of 10 nl/s) was injected either in layer 4 of the primary auditory cortex (A1): anteroposterior, −2.18 mm; lateral, 4.2 mm from bregma; and dorsoventral, 1 mm from the brain surface; or in the internal capsule (IC): anteroposterior, −0.94 mm; lateral, 2.10 mm; dorsoventral, 2.5 mm (Paxinos and Franklin, 2001). The health status of the animals, e.g. healing of the cranial wound and exploratory activity, was checked daily for 7 days after surgery. Then only after full recovery, animals were tested at 7 days after lysolecithin injection when the demyelination effect was maximal and then at 14 and 28 days to test for remyelination (Hall, 1972; Pavelko et al., 1998). Animals matched for age, gender and experimental time point were injected with vehicle solution and served as controls. All injection sites/locations were verified by histochemical staining after the recordings.

2.2. Tissue preparation and immunohistochemistry

Immunohistochemistry was performed on a group of six animals for each time point for the general demyelination and on a group of three animals for the focal demyelination model. Briefly, mice were deeply anesthetized using Foren (isofluran, 1-chloro-2,2,2 trifluoroethyldifluoromethylether; 5% in O_2) and then perfused with 4% paraformaldehyde (PFA) in phosphate buffer via the left cardiac ventricle as previously described (Skripuletz et al., 2008). Brains were removed, postfixed in 4% PFA and paraffin embedded. For light microscopy, 7-µm serial paraffin sections were cut and dried at 37 °C overnight, as described before (Skripuletz et al., 2013). Paraffin embedded sections were dewaxed, rehydrated, and microwaved for 5 min in 10 mM citrate buffer (pH 6.0). Sections were quenched with H_2O_2, blocked for 1 h in phosphate-buffered solution (PBS) containing 3% normal goat serum, 0.1% Triton X-100, and then incubated overnight with the primary antibody. The following primary antibodies were

used: for myelin proteolipid protein (PLP; mouse IgG2a, 1:500, Serotec) and for astrocytes glial fibrillary acidic protein (GFAP; mouse IgG1, 1:200, Millipore). After washing, sections were further incubated with biotinylated anti-mouse IgG (heavy and light chain) secondary antibodies (1:500, Vector Laboratories) for 1 h followed by peroxidase-coupled avidin–biotin complex (ABC Kit, Vector Laboratories). Reactivity was visualized with diamino-3,3′-benzidine (Vector Laboratories). For cell staining, slides were counterstained using Mayer's hemalum solution (Merck). The extent of myelination and astrogliosis was subsequently analyzed by light microscopy (Olympus BX61). In particular, myelin protein-stained sections for PLP were scored using a light microscope (Leica). Scoring of demyelination was performed by three blinded observers, using a scale of 0 (complete lack of myelin) to 4 (normal myelin) (Skripuletz et al., 2008).

Tissue integrity and cellular infiltrates were characterized in paraffin-embedded (Skripuletz et al., 2008) and cryopreserved sections (Göbel et al., 2010) using the following marker: activated microglia were detected using Iba-1 (Wako), GFAP (Sigma) was used as marker for astrocytes, CD3 for T cells. After washing, sections were incubated with the respective secondary antibody for 1 h, followed by peroxidase-coupled ABC Kit (Vector Laboratories, Burlingame, UK) or directly mounted with Mowiol (Calbiochem, San Diego, CA, USA) containing DAPI (Invitrogen, Carlsbad, CA). Cell counting was performed for the following marker: GFAP, Iba-1, and CD3. Immunopositive cells in the auditory cortex and in the internal capsule were counted. Values are presented as number of cells per mm^2.

2.3. Flow cytometry

Flow cytometric analysis of murine peripheral leukocytes was performed as previously described (Ruck et al., 2013). Cells were analyzed on a Gallios Flow Cytometer (Beckman Coulter, Krefeld, Germany). Antibody concentrations were carefully titrated prior to experiments. For flow cytometric evaluation of CNS-invading cells, mice were perfused transcardially with PBS to diminish contamination by leukocytes located within the blood vessels. CNS tissue was dissociated mechanically; followed by an enzymatic digestion with collagenase CLS2 (Worthington, Lakewood, NJ, USA) and DNAse (Sigma Aldrich, Munich, Germany) for 45 min at 37 °C. After two washing steps, the cell suspension was transferred to a 30%/50% Percoll (Amersham, Piscataway, NJ, USA) density gradient. After centrifugation (2500 rpm, 30 min, 20 °C) mononuclear cells were isolated from the interface of the gradient, counted by a Casy® Model TT cell counter (Innovatis AG, Reutlingen, Germany) and stained with appropriate antibodies. The following primary anti-mouse antibodies were used for flow cytometry: the respective isotype controls and CD11b-PerCP-Cy5.5 (clone M1/70) were purchased from BD Biosciences (Heidelberg, Germany); CD3-Brilliant Violet 510 (clone 17A2), CD4-Pacific Blue (clone GK1.5), CD8a-AF700 (clone 53-6.7), CD11b-APC (clone M1/70), CD11c-APC (clone N418), CD25-FITC (clone PC61), CD45-FITC (clone 30-F11), CD69-PE (clone H1.2F3), CD86-PE-Cy7 (clone GL-1), F4/80 (clone BM8) were purchased from Biolegend (Fell, Germany); CD40-PE (clone 1C10), MHC class II (I-A/I-E)-APC-eFluor780 (clone M5/114.15.2) were purchased from eBioscience (San Diego, CA, USA).

2.4. Immunological analysis

Cervical lymph node cells were isolated either from control mice or from cuprizone-treated mice. Cells were stimulated with anti-CD3 (2 μg/ml) and anti-CD28 (1 μg/ml) antibodies. IFNγ and IL-17A levels were assessed by enzyme-linked immunosorbent assay (ELISA, Ready-SET-Go! ELISA kit; eBioscience, Frankfurt, Germany).

For evaluation of cell proliferation, the amount of ATP in the supernatant after cell lysis was assessed as an indicator of cell proliferation using an ATPlite luminescene ATP detection assay system (PerkinElmer, Waltham, USA) according to the manufacturer's instructions. Luminescence was measured on an Infinite 200 PRO multimode microplate reader (Tecan, Switzerland).

2.5. Electrophysiology – in vivo recordings

2.5.1. Electrode implantation

For recording of spontaneous and auditory stimulus-induced unit activities in freely behaving mice, microwire arrays (one array, eight electrodes and one reference/array per brain region; Stablohm 650; California Fine Wire, USA) were implanted under stereotaxic control (David Kopf Instruments, USA). The tip of each wire was gold plated by passing a cathodal current of 1 μA while wires were submerged in a gold solution to reduce the impedance to a range of 150–300 kΩ. Under deep pentobarbital anesthesia (50 mg/kg i.p.), supplemented by subcutaneous injection of carprofen (Rimadyl®; 5 mg/kg), electrodes were implanted in the left hemisphere using the following stereotaxic coordinates (Paxinos and Franklin, 2001): A1 layer 4: anteroposterior −2.18 mm, lateral 4.2 mm from bregma, and dorsoventral 1 mm from the brain surface. Electrodes were fixed with dental cement (Pulpdent-GlassLute, Corporation Watertown, MA; USA). An additional ground electrode was positioned close to the midline over the cerebellar region (5.8/0.5 mm from bregma) in the right hemisphere. The health status of the animals and their recovery, e.g. healing of the cranial wound and exploratory activity, was checked daily for 7 days after surgery. At the end of the experiments, animals were killed by an overdose of pentobarbital (100 mg/kg, i.p), location of the electrode sites were marked by small electrolytic lesions (2.5 mA anodal current for 2 s) and brains were rapidly removed and fixed in 4% phosphate-buffered formaldehyde, pH 7.4. Electrode positions were identified in 50 μM cresyl violet-counterstained coronal brain sections (Fig. 2A) and anatomically located (Supplementary Fig. 2A).

2.5.2. In vivo electrophysiological recordings

After 7–10 days of surgical recovery, recordings of unit activities were performed. In cuprizone-treated mice, recordings were performed at three different time points: after full demyelination (cuprizone in the text), and during early (day 7) and late (day 25) remyelination (Franco-Pons et al., 2007; Skripuletz et al., 2011). Focal demyelination was induced by local lysolecithin injection in A1 and IC. First recordings from focally demyelinated mice were performed 7 days after lysolecithin injection (this group is referred to as day 7 in the text). Next, neuronal activity was recorded during the remyelinating phase (day 14) and following complete remyelination (day 28) (Hall, 1972; Pavelko et al., 1998). Recordings obtained in the same mice prior to lysolecithin injection (day 1) served as control. The recordings were performed before, during, and after the presentation of an auditory stimulus consisting of a sequence with six repetitions of either low- or high-frequency tones (2.5 kHz and 10 kHz at 85 dB, respectively; Fig. 2A). Neuronal activity was recorded with a Multichannel Amplifier System (Alpha Omega, Israel) and stored on a personal computer (IBM). Unit activities were bandpass filtered at 9 kHz, at a sampling rate of 40 kHz. Spikes of individual neurons were sorted by time–amplitude window discrimination and principal component analysis (Offline Sorter, Plexon Inc., Dallas, TX, USA) and verified through quantification of cluster separation, as described before (Narayanan et al., 2011).

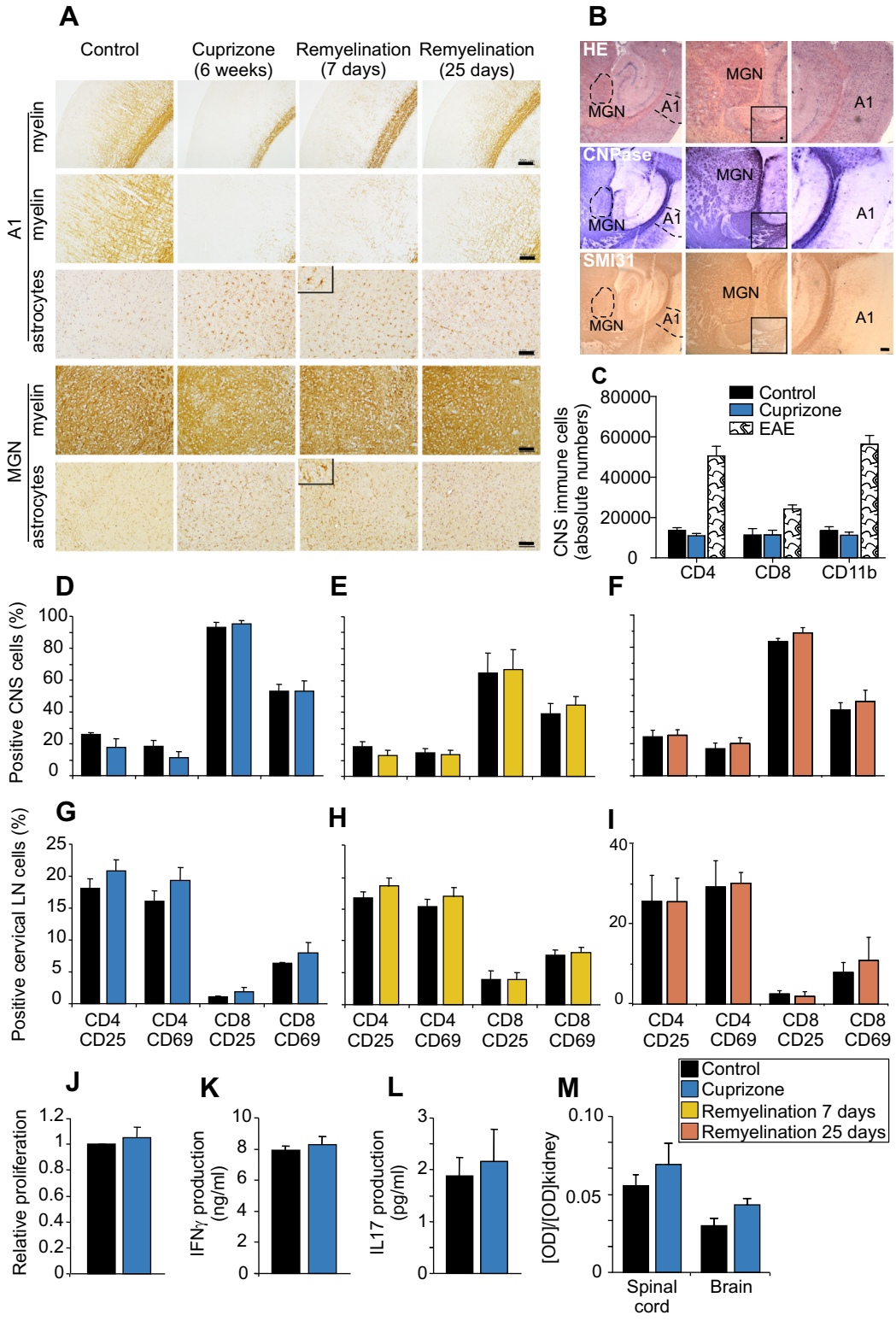

Fig. 1. Cuprizone-induced demyelination is not accompanied by adaptive immune system activation or BBB breakdown. (A) In cuprizone-treated animals, myelin loss, quantified using PLP as marker, was found in the auditory cortex (A1; column 2, rows 1–2) and in the medial geniculate nucleus (MGN; row 5) compared with control. During demyelination, marked time-dependent astrogliosis (GFAP marker) was observed (row 3). (B) Staining with HE, CNPase (adult oligodendrocytes marker), and SMI31 (axonal marker) in acute brain slices containing A1 and MGN. (C) Flow cytometric evaluation of CNS $CD4^+$, $CD8^+$, and $CD11b^+$ cells revealed no differences between controls and cuprizone-treated mice compared to typical EAE-observed values. (D–F) Unaltered activation of CD25 and CD69 markers was observed in CNS-present $CD4^+$ and $CD8^+$ T lymphocytes in cuprizone-treated mice (D), 7 (E) and 25 (F) days after remyelination when compared to age- and gender-matched controls (black bars). (G–I) $CD4^+$ and $CD8^+$ T cells isolated from cervical lymph nodes showed no changes in CD25 and CD69 expression after demyelination (G) and during remyelination (H, I) when compared to age- and gender-matched controls. (J–L) Stimulation with CD3/CD28 showed no changes in proliferative capacity (J) or cytokine production (IFNγ (K)), IL17 (L)). (M) Mouse spinal cord and brain measurements showed no major changes in BBB permeability during remyelination 2 h after i.v. injection of Evans blue. ($n = 5$ for all experiments). Scale bar, 100 μm.

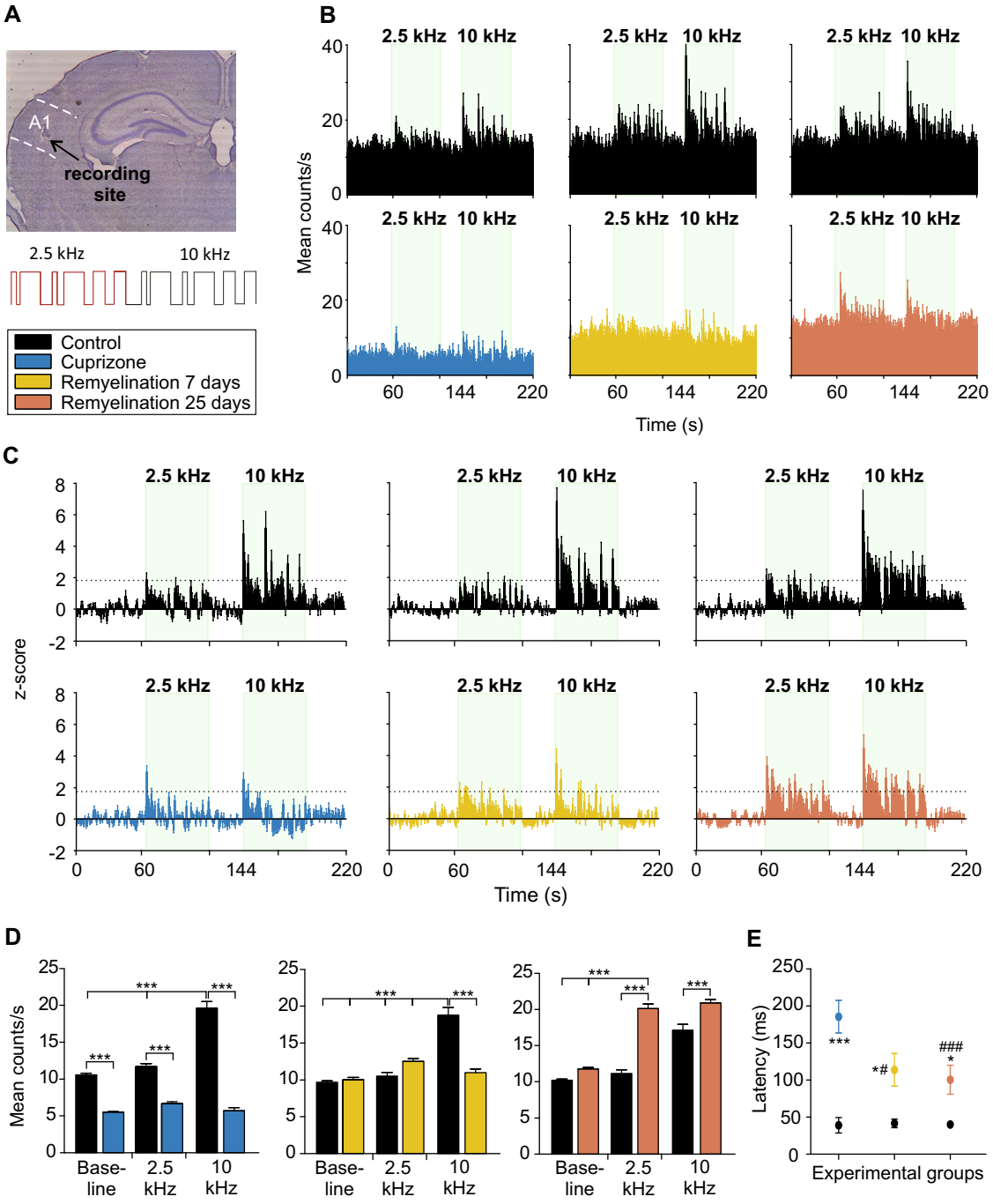

Fig. 2. Myelin loss and restoration influences the auditory thalamocortical pathway functionality. (A) Exemplary coronal brain slice showing the electrode recording site in the layer-4 of A1 and schematic representation of the auditory stimuli protocol. (B) Histograms of the overall neuronal response (bin size = 1 s) to 2.5- and 10-kHz stimuli (green insets), activity is higher in controls (black traces; $n = 43/15$) compared with cuprizone-treated animals ($n = 27/13$; blue traces) and partially restored at 7 ($n = 50/15$; yellow traces) and 25 ($n = 65/16$; magenta traces) days after remyelination. (C) *Z*-score histograms obtained considering only neurons responding to auditory stimulus with a response 1.96 folds higher than baseline (horizontal dashed lines), showed a significantly reduced neuronal activity in cuprizone-treated animals ($n = 20/11$) compared with controls ($n = 20/10$) while the ability to discriminate between tone frequencies is permanently lost (7-day remyelination, $n = 20/9$; 25-day remyelination, $n = 20/13$). (D) Bar graphs quantifying the neuronal stimulus-related firing rate indicated groups and the two frequencies including baseline values ($^{*}p < 0.05$, $^{***}p < 0.001$). (E) The latency to response significantly increased after cuprizone treatment and partially restored 7 and 25 days after remyelination ($^{*}p < 0.05$, $^{***}p < 0.001$ vs. relative controls; $^{\#}p < 0.05$, $^{\#\#\#}p < 0.001$ vs. cuprizone). (For interpretation of the references to colour in this figure legend, the reader is referred to the web version of this article.)

2.5.3. Single-unit analysis

Basal and stimulus evoked activity, as well as *z*-scores of sorted neurons were analyzed by a customized MATLAB routine (The MathWorks). For all analyses except firing-latencies, the time axis of experimental sessions was divided into 1 s bins to calculate firing-rates and z-scores. Firing rates have been calculated as spike-count per second. Values obtained during the first 60 s of an experimental session were defined as baseline activity for every single neuron. Individual firing rates were z-scored to their respective mean baseline activity. Neurons were defined as "responsive" neurons if at least one bin showed z-score $\geqslant 1.96$ in response to stimulus presentation. For analysis of firing-latencies, the time axis of experimental sessions was divided into 0.01 s bins. The latency was defined as the time between the stimulus presentation and the

neuronal response in A1. Analysis was performed by dividing the time axis into 0.01-s bins and by calculating the overall number of spike occurring per bin. Thereafter, the time difference between the time bin of the stimulus onset and the first following time bin showing more than one AP (user-defined threshold) was evaluated. In the text, *n* is given as number of neurons/number of animals recorded.

2.6. Behavioral test

After termination of cuprizone treatment and 25 days after remyelination, mice underwent a modified fear-conditioning protocol to evaluate their ability to discriminate auditory stimulus frequencies: mice (5 per group) were adapted twice to the fear-conditioning apparatus with six neutral tones (unconditioned stimulus CS^-, 2.5 kHz tone, 85 dB, 10-s duration). On the next day, fear conditioning was performed through two trials of three presentations of the conditioned stimulus (CS^+, 10 kHz tone, 85 dB, 9-s duration) paired with an unconditioned stimulus (scrambled foot shock of 0.4 mA, 1-s duration). After 24 h, freezing, namely the percentage of immobility of the animal in response to the conditioned stimulus which is a typical fear-conditioning-related behavior, was taken as readout. Another batch of experiments was performed on the same experimental groups inverting the protocol, with CS^+, 2.5 kHz as the conditioning tone and CS^- 10 kHz as adaptation tone.

The same behavioral paradigm was used in another battery of experiments where animals were injected with lysolecithin either in A1 or IC (6–7 animals per group). Animals were tested using the protocol with 10 kHz as conditioning tone at different time points: 7, 14 and 28 days after lysolecithin injection. Two additional groups were injected with saline either in IC or in A1 and tested 7 days after injection. These animals were considered as control as we observed no serious histopathological damage (see paragraph 3.5) and no behavioral changes at this critical time point after lysolecithin injection.

2.7. Statistics and data analysis

All results are presented as mean ± SEM. Statistical significance was analyzed using One-way ANOVA, factorial ANOVA or mixed designs ANOVAs when both repeated measures and multivariate analysis needed to be performed. Analyses were followed by Bonferroni post hoc tests or by the Least Significant Difference test (LSD) for multiple or pairwise comparisons as specified in the text. For all analyses Statistica (Statsoft, USA), SPSS (IBM Analytics) and Graphpad (Prism 5, GraphPad) were used. Graphs and figures were prepared using Origin, GraphPad, and Coreldraw.

3. Results

3.1. Demyelination induced by cuprizone treatment is not associated with inflammation mediated by the adaptive immune system

By choosing the cuprizone model for general demyelination, we aimed to answer our question concerning the consequences of a general and massive loss of myelin in the central nervous system. Treatment with the copper chelator cuprizone is an established model of general demyelination preferentially targeting mature oligodendrocytes (Matsushima and Morell, 2001; Skripuletz et al., 2011) and inducing demyelination in mice after 5–6 weeks of administration. Staining with the myelin-specific proteolipid protein (PLP) allowed quantification of the myelin content which was reduced in A1 (myelin score: control, 4; cuprizone, 0.67 ± 0.27; $p < 0.01$; Fig. 1A and Supplementary Fig. 1C) as well as in MGN (Fig. 1A) which are parts of a reciprocally connected network including axons and oligodendrocytes (Fig. 1B). The mechanisms underlying cuprizone-induced demyelination, which are not entirely known (Skripuletz et al., 2011), are accompanied by astrocytosis and microglia activation (Fig. 1A and Supplementary Fig. 1A, B). Moreover, no indication of cell infiltration was observed following demyelination. This was especially evident when we compared absolute $CD8^+$, $CD4^+$ and CD11b cell numbers obtained by experimental encephalomyelitis animal models to our experimental groups and controls (Fig. 1C and Supplementary Fig. 1B). Further we analyzed the contribution of different $CD4^+$ and $CD8^+$ population subtypes (CD25 and CD69) to the overall small number of immune cells that we detected in our experimental groups. No signs of inflammation or presence of activation markers of the adaptive immune system were observed following cuprizone treatment compared to respective controls. Termination of the treatment allowed spontaneous remyelination and no signs of inflammation were visible during the early and late phases of remyelination (7 and 25 days, respectively; Fig. 1D–I). In detail, analysis of the effect of time, i.e. the differences between de- and remyelination phases, was not significant for the $CD4^+$ and $CD8^+$ subpopulations in the brain (factorial ANOVA, main effect of time: $F_{(4,26)} = 2.06$, $p = 0.115$ and $F_{(4,26)} = 1.55$, $p = 0.216$, respectively). The analysis of the time effect in immune cell subpopulations isolated from lymphnodes showed no changes during de- and remyelination for the markers CD8/CD25 and CD69 ($F_{(4,26)} = 0.33$, $p = 0.855$) but we observed an effect for CD69 expression on $CD4^+$ T cells ($F_{(4,26)} = 3.54$, $p < 0.05$). This isolated effect could be attributed to differences in the respective control groups and was considered to not be biologically meaningful. Furthermore, no indications of peripheral inflammation (Fig. 1J–L) or blood–brain barrier (BBB) damage were observed (Fig. 1M). Taken together, this approach provided a feasible basis to study the functional consequences mediated by demyelination only, independently from major inflammatory influences.

3.2. General demyelination permanently alters the auditory neuronal network functionality in vivo

After having validated our model, the next step was to investigate the functional consequences of general demyelination by performing *in vivo* electrophysiology in freely behaving animals. We recorded single-unit activity in individual mice from A1 in a longitudinal approach under control conditions, the time of maximal demyelination, and during different phases of remyelination (7, 25 and 45 days in the same animal). Recording electrodes were implanted in layer 4 of A1 (Fig. 2A) in a tonotopic position where neurons are known to respond to frequencies higher than 8 kHz (Hackett et al., 2011; Musacchia et al., 2014). The animals were then exposed to tones of two different frequencies (2.5 and 10 kHz) and neuronal activity was recorded and analyzed (Supplementary Fig. 2A–D). Typical rate histograms showed auditory stimulus-induced peaks of activity on a background of basal activity. In control animals, a sharp increase in activity was evoked by the presentation of the higher frequency stimulus (10 kHz; Fig. 2B, black traces). In the cuprizone-treated animals, the background activity was dramatically reduced with no clear response to auditory stimuli, indicating heavily impaired neuronal network functioning. Interestingly, allowing remyelination in the same animals, during both the early and late phases, partially restored basal activity (Fig. 2B, yellow and magenta traces, respectively) although no clear discrimination between tone frequencies was detectable, namely there were no differences in responsiveness to 2.5 and 10 kHz. Next, we analyzed only the activity of the neurons responding to the stimulus in order to differentiate theirs from the background activity. We achieved that by including in the analysis only neurons showing a significant positive

z-score value at the onset of the auditory stimulus presentation, i.e. the neurons whose significant response ($p \leqslant 0.05$) was 1.96 folds higher than the baseline (z-score $\geqslant 1.96$ to baseline, $p \leqslant 0.05$; indicated in Fig. 2 by horizontal dashed lines). We observed a strong increase in neuronal activity in response to high frequencies (10 kHz; Fig. 2C, black traces and Supplementary Fig. 2B) proving the response specificity and discrimination properties of A1 neurons. Moreover, after cuprizone treatment, the neuronal ability to respond to auditory stimuli was largely reduced at either tested frequency (Fig. 2C, blue traces and Supplementary Fig. 2C). The z-score analysis further indicated a recovery of auditory stimulus-induced activity during all phases of remyelination as the neurons responded to the stimulus. However, no differentiation between stimulus frequencies (2.5 and 10 kHz) was detected (Fig. 2C, yellow and magenta traces, Supplementary Figs. 2D and 3A) suggesting that the ability of the network to discriminate between the two frequencies was lost. These changes were further characterized by stimulus-related firing rate analysis showing a main effect of time (mixed design ANOVA, $F_{(1,171)} = 5.44$, $p = 0.021$), and thus differences between de- and remyeliantion phases. An effect of frequency ($F_{(2,342)} = 73.91$, $p < 0.001$) was also observed interacting with the time domain ($F_{(4,342)} = 4.91$, $p = 0.002$), thereby indicating that changes in the neuronal response during the presentation of the different frequencies were influenced by the different de- and remyelination phases (Fig. 2D). Interestingly, the alterations observed at 25 days of remyelination, persisted also 45 days after remyelination indicating that a prolonged remyelination period does not rescue altered neuronal responses (Supplementary Fig. 3A).

Another parameter often shown to be affected by demyelination is the response latency (Hamada and Kole, 2015; Kim et al., 2013), defined as the time between the presentation of the stimulus and the activation of the corresponding interconnected area which, in our model is A1. In line with the literature, in our study, the response latencies to auditory stimuli for cortical responsive neurons were significantly longer after demyelination (control, 39.04 ± 10.46 ms; cuprizone, 185.58 ± 21.96 ms; $p < 0.001$ vs. respective control) indicating a clear impairment in the ability of the network to convey the information. Again, as shown for the neuronal amplitude, allowing remyelination only partially recovered such impairment during the early (control for day 7, 41.48 ± 5.81 ms; 7-day remyelination, 113.93 ± 21.9 ms) and late phase of remyelination (control for day 25, 40.0 ± 4.41 ms; 25-day remyelination, 100.52 ± 19.59 ms; one-way ANOVA; effect of time: $F_{(2,102)} = 46.65$, $p < 0.001$; pairwise comparisons: 7- and 25-day remyelination vs. respective controls, $p < 0.05$; 7-day remyelination vs. cuprizone, $p < 0.05$; 25-day remyelination vs. cuprizone, $p < 0.01$; Fig. 2E and Supplementary Fig. 3B).

3.3. De- and remyelination alter auditory conditioned behavioral responses in freely behaving animals

To assess the existence of a behavioral correlate between the permanent changes of neuronal activity observed after demyelination and during remyelination, we tested the ability of mice to discriminate different tones in a discriminative auditory Pavlovian conditioning paradigm with freezing as the behavioral readout (Daldrup et al., 2015; Narayanan et al., 2011). Animals were adapted to a 2.5 kHz stimulus and then conditioned with the 10 kHz stimulus coupled to a mild electrical foot shock. Control animals were successfully conditioned and showed significantly higher freezing upon presentation of the conditioned auditory stimulus (10 kHz; control freezing, 63.27 ± 2.34%; Fig. 3A; mixed design ANOVA, effect of frequency: $F_{(1,12)} = 40.36$, $p < 0.001$) compared with the freezing evoked by the presentation of the non-conditioned stimulus (2.5 kHz; control freezing, 20.5 ± 7.35%; $p < 0.001$ vs. 10 kHz; Fig. 3A). The cuprizone-treated mice showed

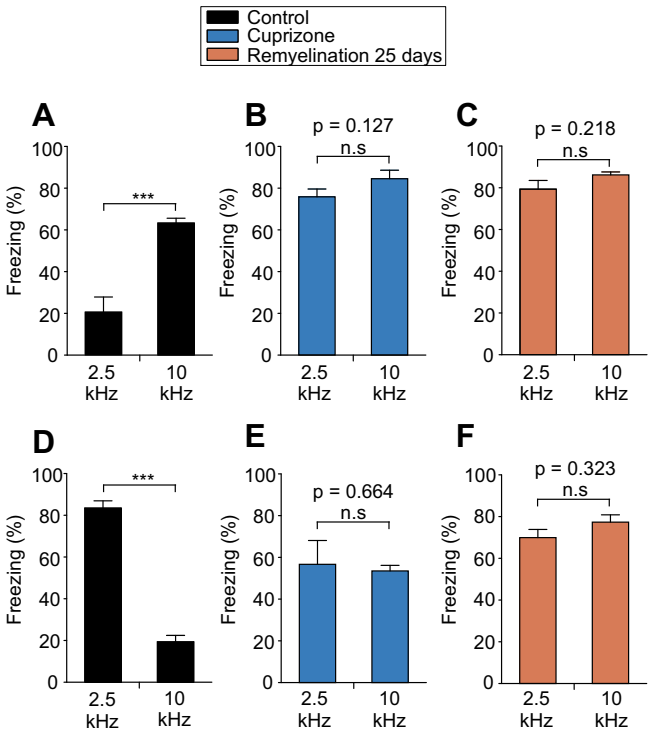

Fig. 3. Altered discrimination responses and freezing behavior as consequence of demyelination. (A) Control animals showed a high percentage of freezing behavior when exposed to the conditioning stimulus (10 kHz) compared with exposure to the unconditioned stimulus (2.5 kHz; $^{***}p < 0.001$; $n = 5$). (B–C) After cuprizone treatment (B) and in the late remyelination phase (C) animals show no differences in the freezing percentage upon presentation of either 2.5- or 10-kHz stimuli. (D–F) Using 10 kHz as unconditioned stimulus and 2.5 kHz as conditioned stimulus, control animals show high freezing in response to the 2.5-kHz but not to the 10-kHz stimulus (D; $^{***}p < 0.001$) while there is no difference in the cuprizone-treated (E) and the remyelinated group (F).

high freezing in response to both stimuli (freezing: 2.5 kHz, 75.84 ± 3.78%; 10 kHz, 84.52 ± 4.11%; $p = 0.127$; Fig. 3B) and the same effect was observed after 25 days of remyelination (freezing: 2.5 kHz, 79.36 ± 4.18%; 10 kHz, 86.25 ± 1.35%; $p = 0.218$; Fig. 3C) suggesting impaired frequency discrimination and indicating that the regrowth of myelin is insufficient to rescue the phenotype (mixed design ANOVA, main effect of time: $F_{(2,12)} = 46.5$, $p < 0.001$ and interaction between time and frequency: $F_{(2,12)} = 15.5$, $p < 0.001$; pairwise comparison shows no differences between cuprizone-treated animals and 25-day remyelination: $p = 0.65$ for 2.5 kHz and $p = 0.67$ for 10 kHz). Very similar results were obtained when the paradigm parameters were inverted, with 2.5 kHz as conditioned stimulus (control freezing: 2.5 kHz, 83.45 ± 3.52%; 10 kHz, 19.38 ± 3.1%; cuprizone freezing: 2.5 kHz, 56.73 ± 11.39%; 10 kHz, 53.51 ± 2.71%; 25-day remyelination freezing: 2.5 kHz, 69.93 ± 9.96%; 10 kHz, 77.36 ± 3.49%; mixed design ANOVA, main effect of time: $F_{(2,12)} = 7.82$, $p = 0.007$ and interaction between time and frequency: $F_{(2,12)} = 28.59$, $p < 0.001$; pairwise comparison: $p < 0.001$ for controls; Fig. 3D–F). Moreover, additional control experiments in which randomly presented high- and low-frequency stimuli of different durations were performed to exclude any learning or pre-existing deficits before behavioral testing (Supplementary Fig. 4A–C).

3.4. Distinct functional consequences of de- and remyelination after lesions in white and cortical gray matter

Having demonstrated that general demyelination heavily impairs neuronal activity in the thalamocortical system and

thereby behavior *in vivo*, our next step was to assess whether focal demyelination of white- or gray matter of the auditory pathway differently impacted network function in a region-specific manner. This approach takes advantage of the ability to mimic typical region-specific pathophysiological lesions observed in human diseases (Muto et al., 2015; Sahin et al., 2015). The more localized gray-matter demyelination events (in comparison to cuprizone-induced events) induced by focal injection of lysolecithin in A1 reduced the response of the A1 neurons to auditory stimuli already at 7 days post injection (z-score $\leqslant 1.96$ to baseline, $p < 0.05$; black traces vs. cyan traces; Fig. 4A, B) with significant differences in the firing rate for every presented frequency and in comparison to the other time points (repeated measures ANOVA, effect of frequency: $F_{(2,38)} = 33{,}39$, $p < 0.001$; pairwise comparison for 10 kHz: 7-day lysolecithin vs. 7-day control: $p = 0.015$; 7-day lysolecithin vs. 14-day lysolecithin: $p = 0.03$ and 7-day lysolecithin vs. 28-day lysolecithin: $p = 0.02$; Supplementary Fig. 5A, B). During remyelination, responses to auditory stimuli were partially restored in A1, while the ability to discriminate different tone frequencies seemed to be permanently lost, as indicated by the z-score and the stimulus-related firing rate analyses at 14 and 28 days post injection (lysolecithin cyan traces vs. control black traces; repeated measures ANOVA, interaction between frequency and time: $F_{(6,114)} = 6.97$, 10 kHz vs. 2.5 kHz at 14-day lysolecithin vs 28-day lysolecithin, $p = 0.23$; Fig. 4A, B and Supplementary Fig. 5A, B). The cortical response latency to auditory stimuli increased 7 days after lysolecithin injection in A1 compared to controls (151.82 ± 16.53 ms vs. 32.33 ± 7.52 ms, respectively; repeated measures ANOVA, $F_{(3,36)} = 21$, $p < 0.001$; Bonferroni post hoc test: $p < 0.001$; Fig. 4E) and was partially restored in the following weeks of remyelination, although not reaching control values (14-day, 85 ± 12 ms; 28-day, 89 ± 12.88 ms; Fig. 4E). In contrast, the focal demyelination of the white matter, specifically in the internal capsule (IC), induced only a transient decrease in A1 neuron responses and relative firing rate upon presentation of all frequencies (7-day, black and purple traces and bars; 7-day baseline vs. 2.5 kHz vs. 10 kHz; Fig. 4C, D and Supplementary Fig. 5C, D) which increased 14 and 28 days post injection (repeated measures ANOVA, effect of frequency: $F_{(2,54)} = 27.44$, $p < 0.001$ and interaction between frequency and time: $F_{(6,162)} = 6.41$, $p = 0.001$; Supplementary Fig. 5C, D) when it reached control (pre-injection-like) values. Accordingly, the latency in A1 was also significantly increased by the demyelination of the IC (control, 38.4 ± 3.20 ms; 7-day lysolecithin IC, 103.24 ± 12.01 ms; repeated measures ANOVA, $F_{(3,69)} = 27.4$, $p < 0.001$; Bonferroni post hoc test, $p < 0.001$ vs. 1-day; Fig. 4F) and control conditions were almost completely restored in the early (14-day, 61.16 ± 2.77 ms; Fig. 4F) and late phase of remyelination (28-day, 38.91 ± 2.79 ms; $p = 1$ vs. 1-day; Fig. 4F).

3.5. Lysolecithin targets myelin and triggers microglia activation

Upon lysolecithin injections, loss and restoration of myelin were clearly observed in acute brain slices stained for the myelin proteolipid protein (PLP) in A1: 7 days after lysolecithin injection, the myelin score decreased (0.33 ± 0.27) compared to control (myelin score, 4) and it increased 28 days after injection even though not reaching control-like values (2.66 ± 0.27; Fig. 5A, first row). Remyelination of white matter lesions was much more efficient than in gray matter lesions: in IC, the myelin score significantly decreased 7 days after lysolecithin injection (1 ± 0.47; $p < 0.05$ vs. control) and finally reached control values 28 days post-injection (3.67 ± 0.27; Fig 5A, third row). In accordance to previous evidence (Jeffery and Blakemore, 1995; Pourabdolhossein et al., 2014), following lysolecithin injection (7 and 14 days after injection), astrocytosis and microglia activation were observed both in A1 and IC as indicated by increased signal for the GFAP (astrocytosis, Fig. 5A, second and fourth row and Fig. 5B) and the Iba1 markers (microglia, Fig. 5B). Of note, weak expression of Iba1 was detected also in the control A1 and IC but it was resting microglia. Indeed, activated microglia is characterized by a different morphology: an amoeboid shape rather than spherical one (Döring et al., 2015; Hall, 1972), as shown in the insets in Fig. 5Ba–e. No signals for the CD3 marker were observed in A1 (data not shown) and very few cells were detected in IC (Fig. 5B). Twenty-eight days after lysolecithin injection, less microglia activation and astrocytosis were observed compared to the previous days (Fig. 5A and B).

3.6. Auditory discrimination abilities are fully restored after remyelination of a white but not a gray matter lesion

In the following, electrophysiological and immunohistological data obtained from focally demyelinated animals were completed by *in vivo* testing. Animals were injected with lysolecithin either in A1 or in IC and tested with the Pavlovian conditioning paradigm for auditory discrimination (see paragraph 2.6) at different time points. Animals were tested 7 days after saline injection and 7, 14 and 28 days after lysolecithin injection. Saline injection, both in A1 and IC did not affect discrimination of auditory stimuli as animals showed significantly higher freezing in response to the conditioned stimulus at 10 kHz (76.38 ± 2.91% and 57.4 ± 7.98% respectively), compared to the non-conditioned stimulus at 2.5 kHz (mixed design ANOVA, A1 effect of frequency, $F_{(1,46)} = 30.29$, $p < 0.001$; IC effect of frequency, $F_{(1,44)} = 109.9$, $p < 0.001$; Fig. 6A and E). Very low levels of freezing were observed 7 days after lysolecithin injection both in A1 (2.5 kHz: 12.13 ± 3.49% and 10 kHz: 12.44 ± 2.63%, Fig. 6B) and IC (2.5 kHz: 12.86 ± 4.2% and 10 kHz: 17.78 ± 0.84%, Fig. 6F) with no significant differences in respect to the presented frequency. Interestingly, in line with the low activity and the lack of discrimination observed with single unit analysis, animals showed low but similar freezing in response to both frequencies 14 days after injection in A1 (2.5 kHz: 23.1 ± 6.96% and 10 kHz: 21.01 ± 6.01%, Fig. 6C). Freezing was increased 28 days after injection in A1 although animals did not distinguish between tones at the two frequencies tested (2.5 kHz: 56.84 ± 2.52% and 10 kHz: 60.51 ± 2.97%, Fig. 6D). This finding is in line with a restored activity but lack of frequency discrimination observed in the single unit analysis. Indeed, a mixed design ANOVA analysis revealed effect of time, i.e. of remyelination for both 2.5 and 10 kHz frequencies with $F_{(3,46)} = 65.15$ and $p < 0.001$ (Post-hoc analysis: saline vs. 7 and 14 days, $p < 0.001$ and vs. 28 days, $p < 0.01$). In contrast, animals showed stimulus-specific behavioral responses similar to those observed under control conditions 14 (2.5 kHz: 23.1 ± 3.33% and 10 kHz: 54.8 ± 3.17%, mixed design ANOVA, effect of time, $F_{(3,44)} = 15.01$, $p < 0.001$; Fig. 6G) and 28 days (2.5 kHz: 17.98 ± 3.33% and 10 kHz: 67.88 ± 6.25%, $p < 0.001$; Fig. 6H) after injection of lysolecithin in the IC. These data indicate recovery of frequency discrimination properties probably mediated by remyelination of white matter lesions.

4. Discussion

When considering the numerous pathological hallmarks characterizing neurodegenerative diseases such as MS, a recurrent event is the loss of myelin (Compston and Coles, 2008; Meuth et al., 2010). Demyelination may occur at early or late stages of the disease and has severe and unpredictable consequences. Proper myelin functioning and plasticity are important for learning new motoric and cognitive tasks in both humans and rodents (Furst

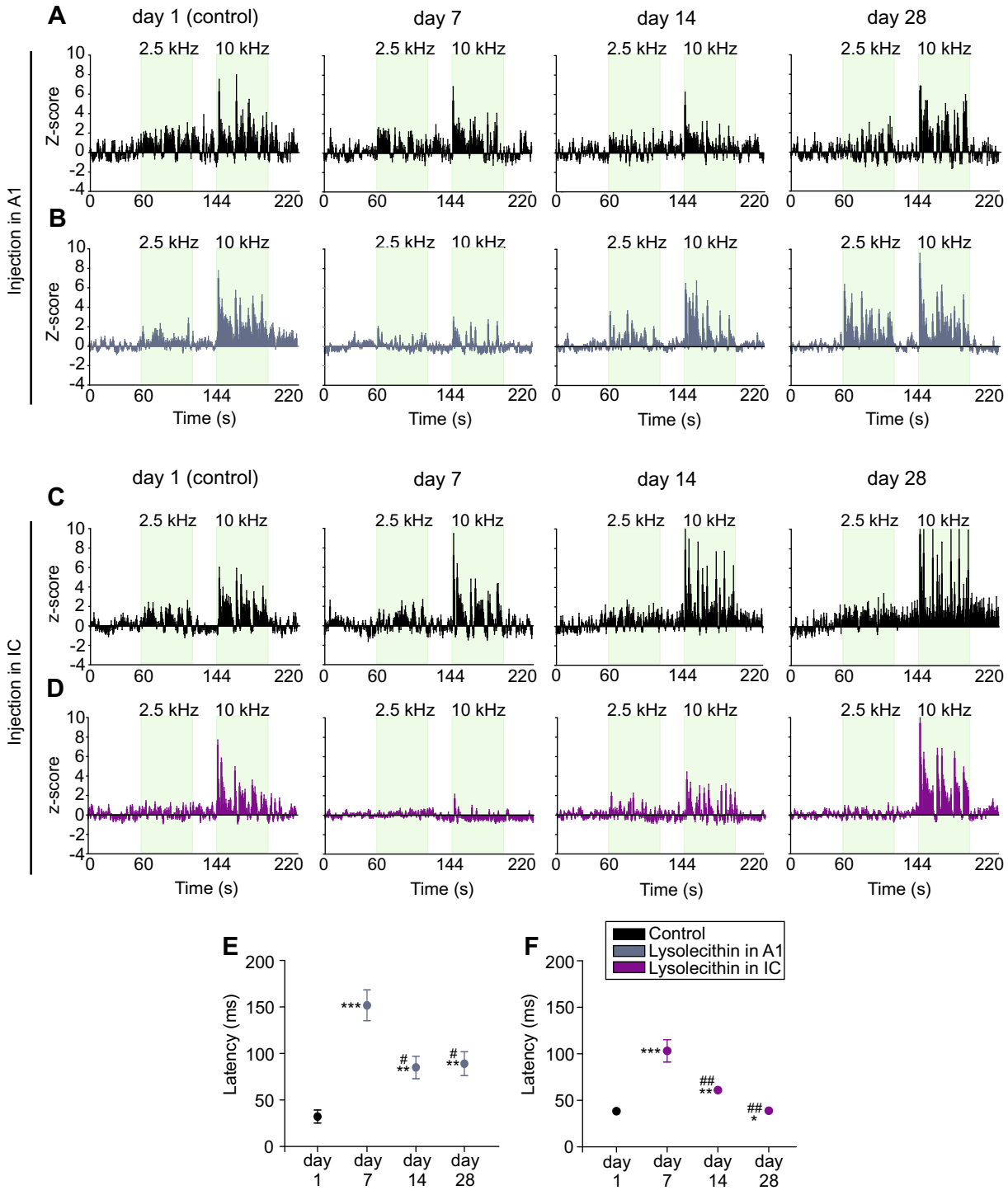

Fig. 4. Focal demyelination permanently affects gray but not white matter. (A–B) Z-score showing impaired neuronal response to 2.5- and 10-kHz stimuli (green insets) 7 days after lysolecithin injection in A1 (n = 31/8; B, cyan traces) compared with saline (n = 6/3; A, black traces) and day 1 (n = 20/8; B, cyan traces). The impairment persists 14 (n = 43/7) and 28 (n = 25/7) days post-injection (B, cyan traces). (C-D) Cortical response decreased 7 days after lysolecithin injection in the IC (D, purple traces; n = 46/9) and fully recovered 14 (n = 36/9) and 28 (n = 43/10) days post-injection, compared with saline (n = 10/5; C, black traces) and day 1 (n = 28/9). (E–F) Latency to response in A1 7, 14 and 28 days after lysolecithin injection in A1 (cyan dots, E) and in IC (purple dots, F; $^{*}p < 0.05$, $^{**}p < 0.01$, $^{***}p < 0.001$ vs. day 1/pre-injection; $^{\#}p < 0.05$ and $^{\#\#}p < 0.01$ vs. 7-day). Scale bar, 100 μm. (For interpretation of the references to colour in this figure legend, the reader is referred to the web version of this article.)

and Levine, 2015; McKenzie et al., 2014; Sahin et al., 2015). Serious cognitive deficits may, therefore, follow demyelination, especially when the damage affects gray matter structures such as cortex and thalamus as occurring in MS pathophysiology (Chang et al., 2012; Mandolesi et al., 2010; Xu et al., 2009). Here already in early disease stages, lesions have been shown to be present additional to the white matter plaques (Deppe et al., 2014, 2013). Considering the recent focus on the thalamocortical system in MS (Calabrese et al., 2015; Matas et al., 2010; Meuth et al., 2010), we aimed to identify consequences of demyelination on neuronal function in the auditory cortex following general and focal demyelination. Subsequently, we examined the role of lesion location by studying

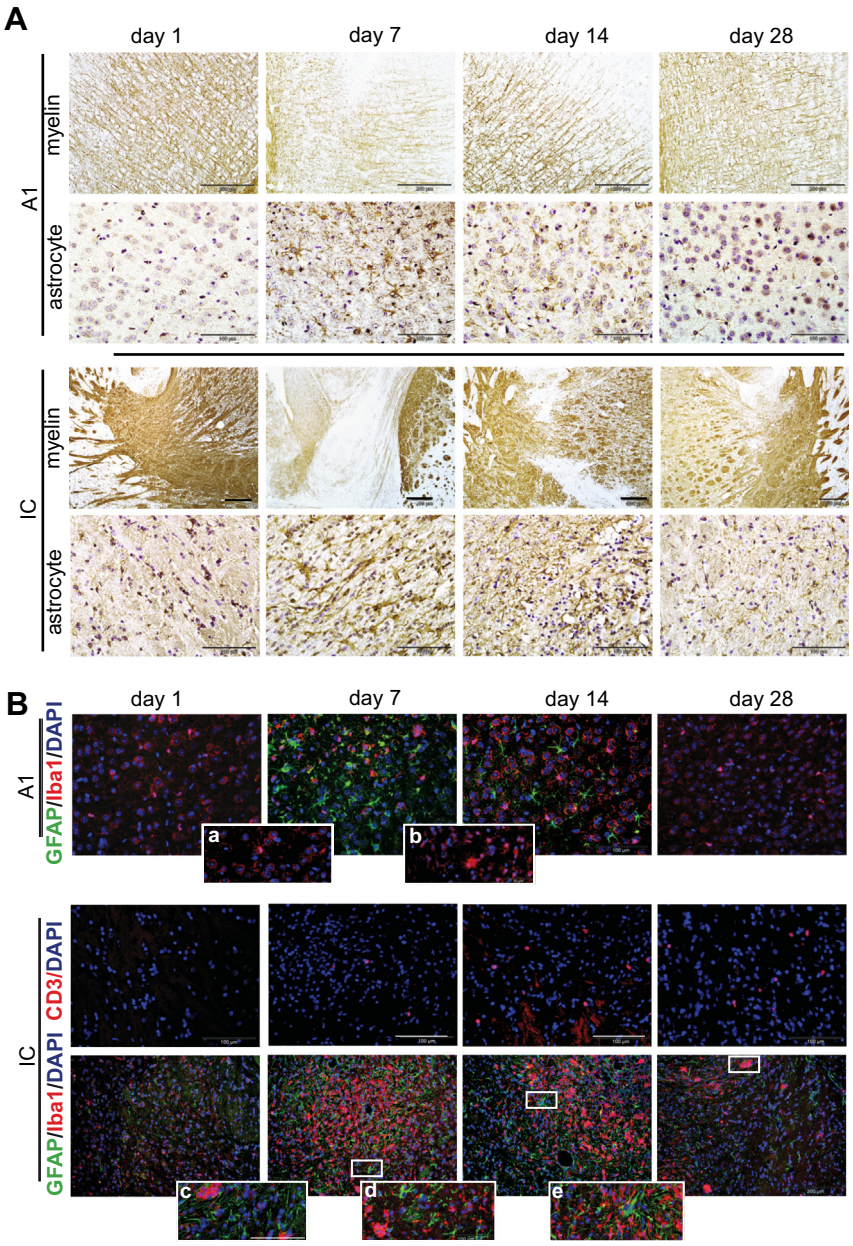

Fig. 5. Lysolecithin injection decreases myelin content and induces atrogliosis. (A) Lysolecithin injections reduced myelin content, quantified using PLP as specific marker, in A1 and IC (first and third row, respectively) already 7 days after injection (second column) compared to control (day 1, first column). 14 and 28 days after injection myelin content increased reaching control-like values only in IC. Lysolecithin injections were associated to astrocytosis both in A1 and IC (second and fourth row) 7 and 14 days after injection (second and third column, respectively). Scale bar PLP: 200 μm and GFAP: 100 μm. (B) Exemplary immunohistological staining for DAPI (marker for cell nuclei, blue), GFAP (marker for astrocytes, green) and Iba1 (marker for macrophage/microglia activation, red) performed at different time points, during control conditions (day 1), and 7, 14 and 28 days after lysolecithin injection. Astrogliosis was observed 7 and 14 days after injection both in A1 and IC (first and third row, respectively). Microglia expression (Iba1, red) was observed also in controls (day 1, first column) but cells did not show typical amoeboid morphology (Ba) characterizing the activated microglia (Bb) in A1 as well as in IC (Bc–e). CD3 cells were detected in a very small number in IC 7, 14 and 28 days after injection (second row). Scale bars A1: 100 μm, 50 μm insets; IC:100 μm and 200 μm. (For interpretation of the references to colour in this figure legend, the reader is referred to the web version of this article.)

the effects of endogenous remyelination in different gray and white matter lesions and concomitantly tested whether the time course of recovery may point to timing strategies of therapeutic intervention. In fact, some previous studies showed that persistent demyelination or remyelination occurring outside a certain time window irreversibly promote axonal damage (Crawford et al., 2009b; Goldschmidt et al., 2009). Accordingly, our overall results show that both localization and timing of lesion appearance and remyelination occurrence affect the length of the disease course and thus call for different times of intervention.

General demyelination following treatment with cuprizone, was associated with loss of frequency-specificity of tone-induced auditory responses and the inability to condition mice to specific tone frequencies in behavioral testing. These changes were not based on brain lymphocyte infiltration or inflammation, even though some astrocytosis and microglial activation were found. Thus, they might be attributed mainly to demyelinating events heavily impairing the neuronal network. By removing cuprizone from the mouse diet we allowed for spontaneous endogenous remyelination (Crawford et al., 2009b; Matsushima and Morell,

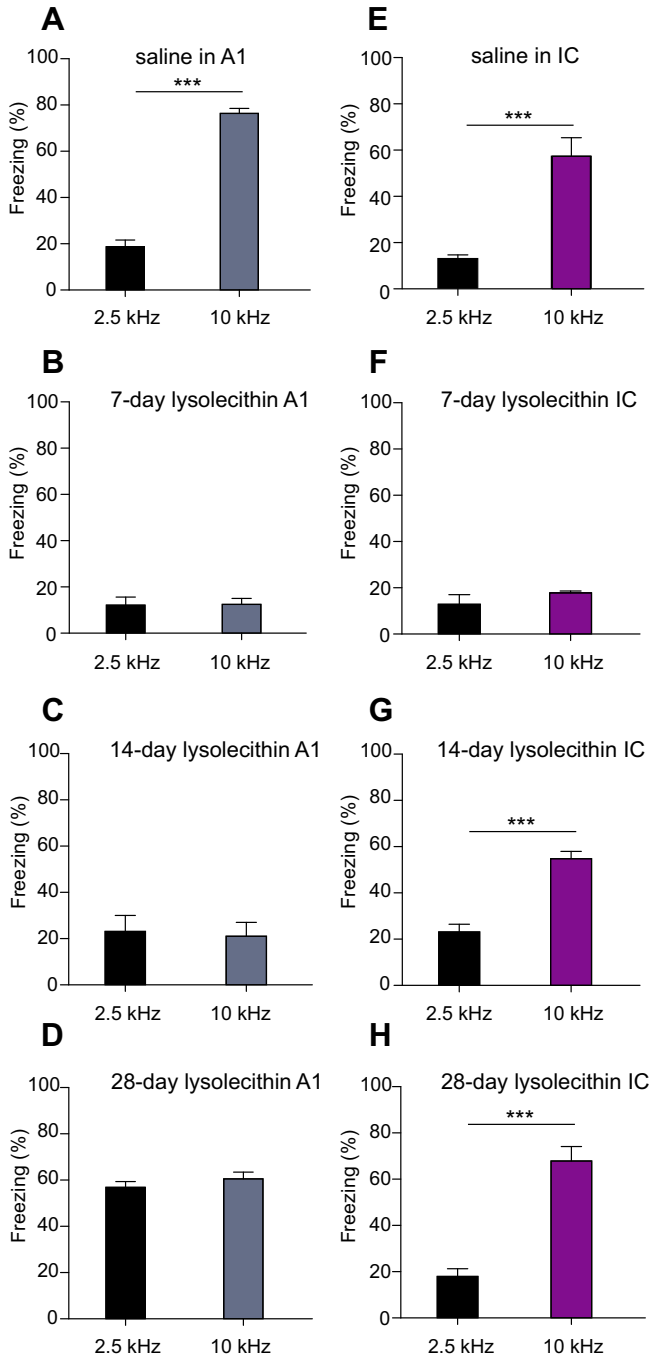

Fig. 6. Remyelination of white matter regions is sufficient to restore the auditory discrimination abilities in freely behaving mice. (A) Animals injected with saline in A1 showed a high percentage of freezing behavior when exposed to the conditioning stimulus (10 kHz) compared with exposure to the unconditioned stimulus (2.5 kHz; $^{***}p < 0.001$; $n = 6$). (B–D) 7 days after lysolecithin injection in A1 (B), as well as 14 (C) and 28 days after (D) animals show no differences in the freezing percentage upon presentation of either 2.5- or 10-kHz stimuli. (E) Animals injected with saline in IC showed a high percentage of freezing behavior when exposed to the conditioning stimulus (10 kHz) compared with exposure to the unconditioned stimulus (2.5 kHz; $^{***}p < 0.001$; $n = 7$). (F–H) 7 days after lysolecithin injection in IC animal showed low freezing response and no differences between the two frequencies (F) while 14 (G) and 28 days after injection (H) they show significant differences in the freezing percentage upon presentation of either 2.5- or 10-kHz stimuli (2.5 kHz vs 10 kHz, $^{***}p < 0.001$).

2001; Skripuletz et al., 2008). Data obtained from histology clearly indicated that myelin was restored: in terms of quantity these values resembled the control values probably mediating the increased neuronal activity that we observed at 7 and 25 days of remyelination in response to auditory stimuli. Previous studies reported that remyelination mainly occurred after an acute exposure to cuprizone (not more than 6 weeks, Matsushima and Morell, 2001) while myelin was not fully reconstituted after a longer exposure to this toxicant (Crawford et al., 2009a; Matsushima and Morell, 2001). It was also shown that already thirty days after removing cuprizone from the diet, myelin reached control-like values which remained stable afterwards (Liebetanz and Merkler, 2006; Matsushima and Morell, 2001; Sachs et al., 2014). In many cases, these stable levels of myelin were associated with locomotor deficits (Zhang et al., 2013) and most strikingly, in our study, these alterations were very clearly reflected by the inability of mice to discriminate between two-tone frequencies in a Pavlovian conditioning paradigm: demyelinated mice could still hear the tone as indicated by a responsive freezing behavior, but this appeared irrespectively of the frequency of the presented tone. Very similar results were obtained at 25 days of remyelination demonstrating that remyelination was insufficient to restore neuronal functionality. Several mechanisms may underlie the partial rescue of the demyelination phenotype: it is known that remyelination is part of a rescue mechanism initiated to protect and regenerate the white matter in the brain (Long and Corfas, 2014). Nevertheless, when this happens after pathological attack, or too late after a given insult, the myelin machinery is probably already seriously compromised and such restoration cannot be fully achieved (Crawford et al., 2009b; Grydeland et al., 2013; Rodgers et al., 2013). In fact, following demyelination a number of consequent events occur to alter both myelin and neurons (Hirrlinger and Nave, 2014). Oligodendrocyte death due to lack of metabolic support which is normally provided by astrocytes affects neuronal survival and axonal functioning (Nave and Werner, 2014; Skripuletz et al., 2013). The disappearance of myelin wraps around the axon lead to an altered expression of some ion channels i.e. $Na_v1.2$, $Na_v1.8$ and Kv7.3 channels, whose correct functionality is important for maintaining cell excitability (Bouafia et al., 2013; Crawford et al., 2009b; Hamada and Kole, 2015). Furthermore, it may be very difficult to discriminate between purely neuron- or oligodendrocyte-mediated mechanisms due to their highly interdependent cross talk.

At the same time, our data highlighted the importance of timing and location of lesions to allow remyelination accompanied by amelioration of discrimination properties in the auditory cortex. By pharmacologically targeting white or gray matter regions with lysolecithin we considered the "regionality" factor. Lysolecithin is known to induce oligodendrocyte death, astrocytosis and microglia activation thereby leading to transient demyelination. The latter is followed by spontaneous remyelination promoted by oligodendrocytes progenitors (OPCs) that can access the targeted area after the compound is metabolized and the debris of old myelin removed by macrophages (Hall, 1972; Pavelko et al., 1998). MS pathophysiology is characterized by defined and local lesions in the thalamocortical system rather than a diffused general demyelination (Calabrese et al., 2015; Deppe et al., 2016; Minagar et al., 2013) and, via local lysolecithin injections we aimed at mimicking this pathological feature more accurately. The focal demyelination decreased neuronal activity recorded in A1 upon auditory stimulus presentation when lysolecithin was injected into A1 and IC in a very similar way (Fig. 7C1 and D1). But, interestingly, during the remyelination phase, we observed complete recovery of the system, with regard to neuronal response, frequency discrimination *in vivo*, 28 days after injection when solely the IC was targeted. In contrast, no functional positive effect of remyelination was observed for the discrimination abilities of the cortical neurons when A1 was affected (Fig. 7C1 and C2). This outcome indicates that the positive effect of spontaneous remyelination, which could

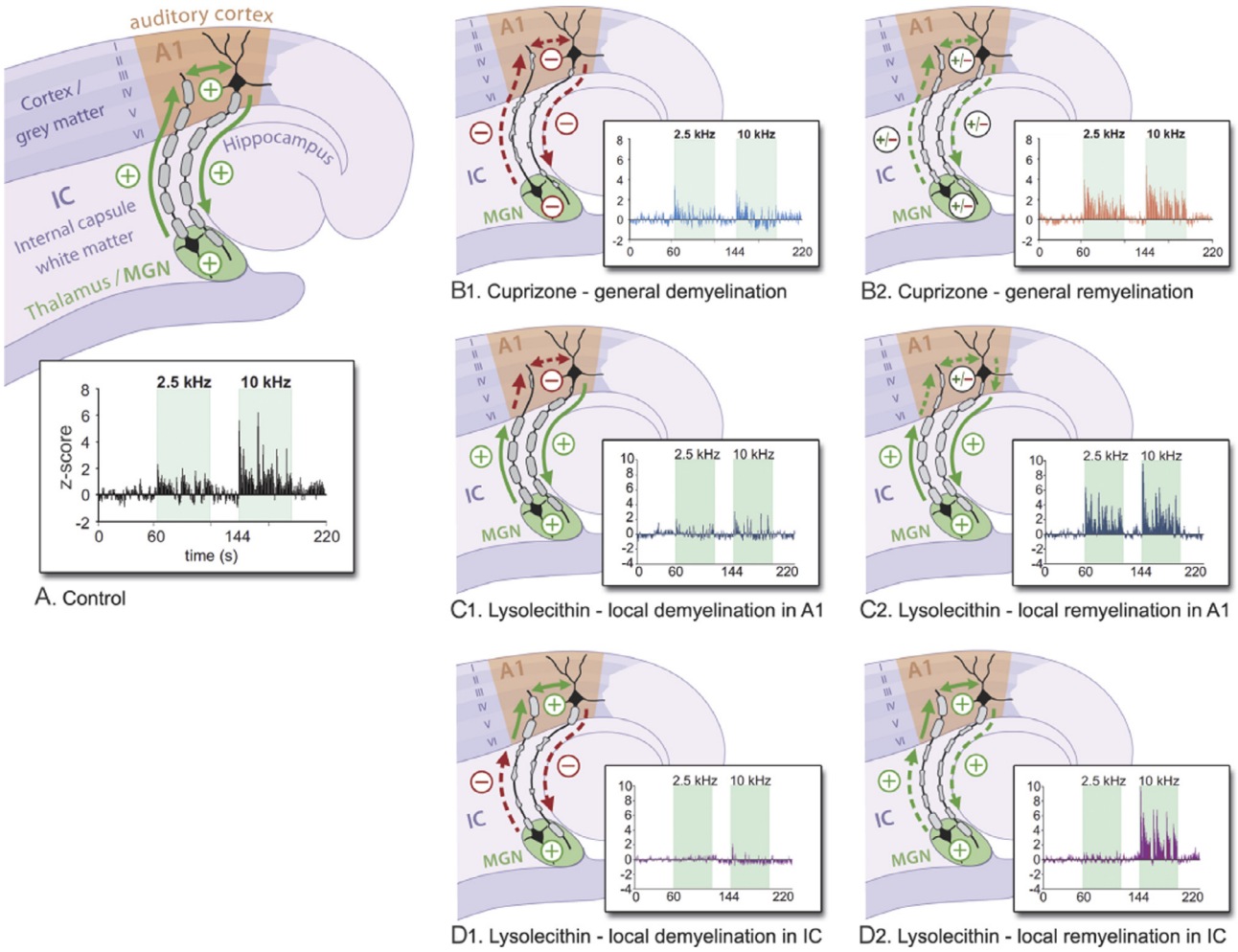

Fig. 7. Graphic summary of the effects of general and focal de- and remyelination in A1. (A) Schematic representation of a well-functioning auditory thalamocortical pathway, as indicated by the green arrows and the positive sign (+), with intact myelin organization and physiological cortical single-unit response. Cuprizone-induced general (B1) and focal demyelinated lesions induced by lysolecithin injection in A1 (gray matter; C1) or in IC (white matter; D1), dramatically decreased cortical neuronal response to any stimulus (electrical or auditory one), as indicated by the dashed-red arrows and the negative sign (−). General remyelination (B2) and cortical focal remyelination after A1 lysolecithin-induced lesion (C2) are accompanied by a restored neuronal activity but permanent loss of frequency-discrimination abilities in response to an auditory stimulus (dashed green arrows and the sign (+/−)). In contrast, the focal remyelination occurring after a lysolecithin-induced IC (white matter) lesion was associated with both restored activity and discriminatory skills in A1 (green dashed arrows and the sign (+); D2). (For interpretation of the references to colour in this figure legend, the reader is referred to the web version of this article.)

be considered as a test for "remyelination strategies" (Crawford et al., 2009b), was region- and time-specific. In fact, the phenotype was rescued only after 28 days (and not at intermediate time points), but this only happened when solely the white matter was affected. Moreover, the gray matter lesion in A1 showed a functional course similar to the cuprizone-treated animals elucidating the importance of the spatiotemporal characteristics of lesions. After all, general demyelination affected both white matter integrity and gray matter functionality (Crawford et al., 2009b; Hamada and Kole, 2015). Thus, not only local cortico-cortical circuits were affected but also long-range connections to many subcortical regions that could have contributed to the heavily impaired cortical network function (Crawford et al., 2009b; Tewarie et al., 2014a,b). Therefore, this would suggest a regulation of neuronal function by axonal myelination or vice versa, thereby supporting the concept of interaction between myelin turnover and axonal activity (Yeung et al., 2014). In line with these findings, the fine tuning of myelination processes, like the correct migration of oligodendrocyte progenitor cells, was shown to be fundamental for learning and consolidating new motor tasks (McKenzie et al., 2014). Also learning new tasks and acquiring new skills simultaneously promotes myelination itself and the maintenance of a functioning myelin machinery (Sampaio-Baptista et al., 2013). In this regard, the loss of myelin in the cuprizone model could mediate the inability of the animals to discriminate between the tones and their high percentage of freezing. In fact, the loss of myelin would affect the directionality of the incoming stimulus as well as cortico-cortical connections of the local auditory circuit of A1 which is involved in the fine tuning of different frequencies (Groh et al., 2014; Hackett et al., 2011; Musacchia et al., 2014). Therefore the behavioral changes observed even after remyelination suggest a persistent impairment of the neuronal network deriving from an alteration of the cortico-cortical connection and/or the activation of compensatory mechanisms, likely involving sub-cortical auditory-related regions (Groh et al., 2014) thereby pointing to a dominant role played by gray matter regions in general. This hypothesis is supported by the observed functional consequences of white and gray matter lesions in lysolecithin-injected animals. A remyelinated white matter lesion was associated with functional restoration of auditory discrimination capabilities in mice. On the contrary, gray matter lesions were associated with permanent auditory frequency discrimination loss.

Previous evidence has suggested a link between gray matter damage and the onset of cognitive and motor deficits (Calabrese et al., 2009; Gamboa et al., 2014; Tewarie et al., 2014a,b). Nevertheless, the diagnosis, location and handling of white and/or gray matter lesions and their functional consequences, are an ongoing issue of debate (Parisi et al., 2014). In earlier days, white matter lesions were considered the hallmark for diagnosis of MS in patients (Hulst and Geurts, 2011) and were the earliest characteristics to be clinically detected (Parisi et al., 2014) mainly because functional deficits leading to consultation normally appear later in the disease course or they were difficult to associate to it (Benedict et al., 2004). In some cases, such association was so unlikely that physicians talked about a cortical MS disease, a parallel disease mainly characterized by functional cognitive and locomotor deficits (Riccitelli et al., 2011; Zarei et al., 2003). Nowadays, gray matter lesions are identified at early stages of the disease (Deppe et al., 2016; Fleischer et al., 2016) due to more advanced technological approaches. Moreover, besides damaged gray matter regions, episodes of atrophy and cortical thinning were observed so that they are also considered as disease hallmarks (Calabrese et al., 2010; Vercellino et al., 2005). Therefore a large number of functional consequences of cortical damage have to be considered. Alterations of the cortico-cortical connections and white/gray matter disruption were associated with changes in neuronal clustering within the cortex and were postulated to underlie altered neuronal excitability in MS and Alzheimer's patients, as well in animal models of neurodegeneration, (Fleischer et al., 2016; Ghaffarian et al., 2016; Markoullis et al., 2012; Sutor et al., 2000; Villain et al., 2010). In our case, such reorganization would indeed have important consequences given the strict topographic and tonotopic organization of the neurons in A1 (Hackett et al., 2011; Musacchia et al., 2014). Interestingly, fMRI studies in MS patients revealed hierarchical alterations of cortex and interconnected subcortical regions which were related to altered neuronal network functioning and cognitive impairment (Gamboa et al., 2014; He et al., 2009; Sanfilipo et al., 2006; Tewarie et al., 2014a,b) and, similar to rodents, cortical structural alterations were associated with the onset of cognitive and motor deficits (Nave and Werner, 2014; Zhou et al., 2013).

Despite advanced techniques for diagnosis, broad availability of different drugs and new basic or clinical research aiming to identify, distinguish and characterize the two types of lesions, the reciprocal causality of the appearance of the white and gray matter lesions (Bodini et al., 2016; De Stefano et al., 2003) and their functional correlation (Bo et al., 2007) remain unclear. Assessing whether a damaged cortex influences myelin functionality or if a white matter lesion triggers the occurrence of gray matter damage is challenging.

5. Conclusion

In conclusion, it is important to consider the clinical implications and the translational potential of the findings we describe herein. The evidence that a gray matter lesion exerts different functional consequences compared to a white matter lesion is a significant observation with profound implications for those patients diagnosed with severe gray matter damage. The successful recovery of function following remyelination of white matter lesions might give important hints to the mechanisms of action of novel treatment options for MS, such as anti-LINGO, an antibody directed against the LINGO-1 protein which inhibits myelin synthesis (Agúndez et al., 2015; Inoue et al., 2007; Rudick et al., 2008). The first trial with patients affected by optic neuritis (ON) was able to show a significant decrease of visual-evoked potential latencies in the anti-LINGO1 group compared to the control group. ON is mainly characterized by demyelination and this strongly supports the conclusion that promoting remyelination seems to be the right approach in cases of white matter damage (Biogen's anti-LINGO promises nerve repair, 2015; Mullard, 2016). Moreover, the insights of our study might help to select eligible patients, who will benefit the most from these new therapies. We believe that our approach can be used as a tool or a model providing a conceptual framework to understand the mechanisms of action of existing drugs, to assist new drug discovery and to develop individualized diagnostic and therapeutic strategies based on the characterization of lesions and the timing of intervention.

Author contributions

MC and VN designed and ran experiments. VN designed, performed, and analyzed the *in vivo* experiments. MC, SGM, TB, VN, HCP wrote the manuscript. KG, MS, VG, TSk, and AMH performed the immunohistological evaluation. SB and TR performed and analyzed the FACS assays. TSe helped in designing and analyzing the *in vivo* experiments. PM wrote the MATLAB routines used for analysis together with TD. CK and PE helped revising the manuscript. SGM, TB, HCP, and HW designed and supervised the project. All authors approved the final version of the manuscript.

Competing financial interest

The authors declare no conflict of interest.

Acknowledgments

We would like to thank Birgit Herrenpoth, Svetlana Kiesling, Julia Schröer, Petra Berenbrock, Hubert Bäumer, Frank Kurth, Jeannette Budde, Carina Butz and Katharina Fricke for excellent technical assistance. We would also like to thank Dr. Hanna Szkudlarek, Dr. Mehrnoush Zobeiri and Dr. Jörg Lesting for the fruitful discussions and support of the project. We would like to thank Heike Blum, our excellent medical illustrator. This study was supported by the German Research Foundation (DFG; CRC SFB-128, B06 Meuth/Budde/Pape; ME3283/5-1) and by Biogen Idec and Novartis grants.

Appendix A. Supplementary data

Supplementary data associated with this article can be found, in the online version, at http://dx.doi.org/10.1016/j.bbi.2016.08.014.

References

Agúndez, J.A., Jiménez-Jimenez, F.J., Alonso-Navarro, H., García-Martín, E., 2015. The potential of LINGO-1 as a therapeutic target for essential tremor. Expert Opin. Ther. Targets 19, 1139–1148. http://dx.doi.org/10.1517/14728222.2015.1028360.

Benedict, R.H.B., Carone, D.A., Bakshi, R., 2004. Correlating brain atrophy with cognitive dysfunction, mood disturbances, and personality disorder in multiple sclerosis. J. Neuroimag. 14, 36S–45S. http://dx.doi.org/10.1111/j.1552-6569.2004.tb00277.x.

Bhatt, A., Fan, L.-W., Pang, Y., 2014. Strategies for myelin regeneration: lessons learned from development. Neural Regen. Res. 9, 1347–1350. http://dx.doi.org/10.4103/1673-5374.137586.

Biogen's anti-LINGO promises nerve repair, 2015. Nat. Biotechnol. 33. http://dx.doi.org/10.1038/nbt0615-573b, 573–573..

Bo, L., Geurts, J.J., van der Valk, P., Polman, C., Barkhof, F., 2007. Lack of correlation between cortical demyelination and white matter pathologic changes in multiple sclerosis. Arch. Neurol. 64, 76–80. http://dx.doi.org/10.1001/archneur.64.1.76.

Bodini, B., Chard, D., Altmann, D.R., Tozer, D., Miller, D.H., Thompson, A.J., Wheeler-Kingshott, C., Ciccarelli, O., 2016. White and gray matter damage in primary progressive MS: the chicken or the egg? Neurology 86, 170–176. http://dx.doi.org/10.1212/WNL.0000000000002237.

Bouafia, A., Golmard, J.-L., Thuries, V., Sazdovitch, V., Duyckaerts, C., Hauw, J.J., Fontaine, B., Seilhean, D., 2013. Axonal expression of sodium channels and

neuropathology of the plaques in multiple sclerosis. Neuropathol. Appl. Neurobiol. http://dx.doi.org/10.1111/nan.12059.
Calabrese, M., Agosta, F., Rinaldi, F., Mattisi, I., Grossi, P., Favaretto, A., Atzori, M., Bernardi, V., Barachino, L., Rinaldi, L., Perini, P., Gallo, P., Filippi, M., 2009. Cortical lesions and atrophy associated with cognitive impairment in relapsing-remitting multiple sclerosis. Arch. Neurol. 66, 1144–1150. http://dx.doi.org/10.1001/archneurol.2009.174.
Calabrese, M., Magliozzi, R., Ciccarelli, O., Geurts, J.J.G., Reynolds, R., Martin, R., 2015. Exploring the origins of grey matter damage in multiple sclerosis. Nat. Rev. Neurosci. 16, 147–158. http://dx.doi.org/10.1038/nrn3900.
Calabrese, M., Rinaldi, F., Mattisi, I., Grossi, P., Favaretto, A., Atzori, M., Bernardi, V., Barachino, L., Romualdi, C., Rinaldi, L., Perini, P., Gallo, P., 2010. Widespread cortical thinning characterizes patients with MS with mild cognitive impairment. Neurology 74, 321–328. http://dx.doi.org/10.1212/WNL.0b013e3181cbcd03.
Chang, A., Staugaitis, S.M., Dutta, R., Batt, C.E., Easley, K.E., Chomyk, A.M., Yong, V.W., Fox, R.J., Kidd, G.J., Trapp, B.D., 2012. Cortical remyelination: a new target for repair therapies in multiple sclerosis. Ann. Neurol. 72, 918–926. http://dx.doi.org/10.1002/ana.23693.
Compston, A., Coles, A., 2008. Multiple sclerosis. Lancet 372, 1502–1517. http://dx.doi.org/10.1016/S0140-6736(08)61620-7.
Crawford, D.K., Mangiardi, M., Tiwari-Woodruff, S.K., 2009a. Assaying the functional effects of demyelination and remyelination: revisiting field potential recordings. J. Neurosci. Methods 182, 25–33. http://dx.doi.org/10.1016/j.jneumeth.2009.05.013.
Crawford, D.K., Mangiardi, M., Xia, X., López-Valdés, H.E., Tiwari-Woodruff, S.K., 2009b. Functional recovery of callosal axons following demyelination: a critical window. Neuroscience 164, 1407–1421. http://dx.doi.org/10.1016/j.neuroscience.2009.09.069.
Daldrup, T., Remmes, J., Lesting, J., Gaburro, S., Fendt, M., Meuth, P., Kloke, V., Pape, H.-C., Seidenbecher, T., 2015. Expression of freezing and fear-potentiated startle during sustained fear in mice. Genes. Brain. Behav. http://dx.doi.org/10.1111/gbb.12211.
De Stefano, N., Matthews, P.M., Filippi, M., Agosta, F., De Luca, M., Bartolozzi, M.L., Guidi, L., Ghezzi, A., Montanari, E., Cifelli, A., Federico, A., Smith, S.M., 2003. Evidence of early cortical atrophy in MS: relevance to white matter changes and disability. Neurology 60, 1157–1162. http://dx.doi.org/10.1212/01.WNL.0000055926.69643.03.
Deppe, M., Krämer, J., Tenberge, J.-G., Marinell, J., Schwindt, W., Deppe, K., Groppa, S., Wiendl, H., Meuth, S.G., 2016. Early silent microstructural degeneration and atrophy of the thalamocortical network in multiple sclerosis. Hum. Brain Mapp. http://dx.doi.org/10.1002/hbm.23144.
Deppe, M., Marinell, J., Krämer, J., Duning, T., Ruck, T., Simon, O.J., Zipp, F., Wiendl, H., Meuth, S.G., 2014. Increased cortical curvature reflects white matter atrophy in individual patients with early multiple sclerosis. NeuroImage. Clin. 6, 475–487. http://dx.doi.org/10.1016/j.nicl.2014.02.012.
Deppe, M., Müller, D., Kugel, H., Ruck, T., Wiendl, H., Meuth, S.G., 2013. DTI detects water diffusion abnormalities in the thalamus that correlate with an extremity pain episode in a patient with multiple sclerosis. NeuroImage. Clin. 2, 258–262. http://dx.doi.org/10.1016/j.nicl.2013.01.008.
Döring, A., Sloka, S., Lau, L., Mishra, M., van Minnen, J., Zhang, X., Kinniburgh, D., Rivest, S., Yong, V.W., 2015. Stimulation of monocytes, macrophages, and microglia by amphotericin B and macrophage colony-stimulating factor promotes remyelination. J. Neurosci. 35, 1136–1148. http://dx.doi.org/10.1523/JNEUROSCI.1797-14.2015.
Fleischer, V., Groger, A., Koirala, N., Droby, A., Muthuraman, M., Kolber, P., Reuter, E., Meuth, S.G., Zipp, F., Groppa, S., 2016. Increased structural white and grey matter network connectivity compensates for functional decline in early multiple sclerosis. Mult. Scler. J. http://dx.doi.org/10.1177/1352458516651503.
Franco-Pons, N., Torrente, M., Colomina, M.T., Vilella, E., 2007. Behavioral deficits in the cuprizone-induced murine model of demyelination/remyelination. Toxicol. Lett. 169, 205–213. http://dx.doi.org/10.1016/j.toxlet.2007.01.010.
Franklin, R.J.M., ffrench-Constant, C., Edgar, J.M., Smith, K.J., 2012. Neuroprotection and repair in multiple sclerosis. Nat. Rev. Neurol. 8, 624–634. http://dx.doi.org/10.1038/nrneurol.2012.200.
Franklin, R.J.M., Gallo, V., 2014. The translational biology of remyelination: past, present, and future. Glia 62, 1905–1915. http://dx.doi.org/10.1002/glia.22622.
Furst, M., Levine, R.A., 2015. Hearing disorders in multiple sclerosis. Handb. Clin. Neurol. 129, 649–665. http://dx.doi.org/10.1016/B978-0-444-62630-1.00036-6.
Gamboa, O.L., Tagliazucchi, E., von Wegner, F., Jurcoane, A., Wahl, M., Laufs, H., Ziemann, U., 2014. Working memory performance of early MS patients correlates inversely with modularity increases in resting state functional connectivity networks. Neuroimage 94, 385–395. http://dx.doi.org/10.1016/j.neuroimage.2013.12.008.
Ghaffarian, N., Mesgari, M., Cerina, M., Göbel, K., Budde, T., Speckmann, E.-J., Meuth, S.G., Gorji, A., 2016. Thalamocortical-auditory network alterations following cuprizone-induced demyelination. J. Neuroinflamm. 13, 160. http://dx.doi.org/10.1186/s12974-016-0629-0.
Göbel, K., Melzer, N., Herrmann, A.M., Schuhmann, M.K., Bittner, S., Ip, C.W., Hünig, T., Meuth, S.G., Wiendl, H., 2010. Collateral neuronal apoptosis in CNS gray matter during an oligodendrocyte-directed CD8(+) T cell attack. Glia 58, 469–480. http://dx.doi.org/10.1002/glia.20938.
Goldschmidt, T., Antel, J., König, F.B., Brück, W., Kuhlmann, T., 2009. Remyelination capacity of the MS brain decreases with disease chronicity. Neurology 72, 1914–1921. http://dx.doi.org/10.1212/WNL.0b013e3181a8260a.
Groh, A., Bokor, H., Mease, R.A., Plattner, V.M., Hangya, B., Stroh, A., Deschenes, M., Acsády, L., 2014. Convergence of cortical and sensory driver inputs on single thalamocortical cells. Cereb. Cortex 24, 3167–3179. http://dx.doi.org/10.1093/cercor/bht173.
Grydeland, H., Walhovd, K.B., Tamnes, C.K., Westlye, L.T., Fjell, A.M., 2013. Intracortical myelin links with performance variability across the human lifespan: results from T1- and T2-weighted MRI myelin mapping and diffusion tensor imaging. J. Neurosci. 33, 18618–18630. http://dx.doi.org/10.1523/JNEUROSCI.2811-13.2013.
Hackett, T.A., Barkat, T.R., O'Brien, B.M.J., Hensch, T.K., Polley, D.B., 2011. Linking topography to tonotopy in the mouse auditory thalamocortical circuit. J. Neurosci. 31, 2983–2995. http://dx.doi.org/10.1523/JNEUROSCI.5333-10.2011.
Hall, S.M., 1972. The effect of injections of lysophosphatidyl choline into white matter of the adult mouse spinal cord. J. Cell Sci. 10, 535–546.
Hamada, M.S., Kole, M.H.P., 2015. Myelin loss and axonal ion channel adaptations associated with gray matter neuronal hyperexcitability. J. Neurosci. 35, 7272–7286. http://dx.doi.org/10.1523/JNEUROSCI.4747-14.2015.
He, Y., Dagher, A., Chen, Z., Charil, A., Zijdenbos, A., Worsley, K., Evans, A., 2009. Impaired small-world efficiency in structural cortical networks in multiple sclerosis associated with white matter lesion load. Brain 132, 3366–3379. http://dx.doi.org/10.1093/brain/awp089.
Hirrlinger, J., Nave, K.-A., 2014. Adapting brain metabolism to myelination and long-range signal transduction. Glia 62, 1749–1761. http://dx.doi.org/10.1002/glia.22737.
Hulst, H.E., Geurts, J.J.G., 2011. Gray matter imaging in multiple sclerosis: what have we learned? BMC Neurol. 11, 153. http://dx.doi.org/10.1186/1471-2377-11-153.
Hulst, H.E., Steenwijk, M.D., Versteeg, A., Pouwels, P.J.W., Vrenken, H., Uitdehaag, B.M.J., Polman, C.H., Geurts, J.J.G., Barkhof, F., 2013. Cognitive impairment in MS: impact of white matter integrity, gray matter volume, and lesions. Neurology 80, 1025–1032. http://dx.doi.org/10.1212/WNL.0b013e31828726cc.
Inoue, H., Lin, L., Lee, X., Shao, Z., Mendes, S., Snodgrass-Belt, P., Sweigard, H., Engber, T., Pepinsky, B., Yang, L., Beal, M.F., Mi, S., Isacson, O., 2007. Inhibition of the leucine-rich repeat protein LINGO-1 enhances survival, structure, and function of dopaminergic neurons in Parkinson's disease models. Proc. Natl. Acad. Sci. U. S. A. 104, 14430–14435. http://dx.doi.org/10.1073/pnas.0700901104.
Jeffery, N.D., Blakemore, W.F., 1995. Remyelination of mouse spinal cord axons demyelinated by local injection of lysolecithin. J. Neurocytol. 24, 775–781.
Kilkenny, C., Browne, W., Cuthill, I.C., Emerson, M., Altman, D.G., 2010. Animal research: reporting in vivo experiments: the ARRIVE guidelines. Br. J. Pharmacol. 160, 1577–1579. http://dx.doi.org/10.1111/j.1476-5381.2010.00872.x.
Kim, J.H., Renden, R., von Gersdorff, H., 2013. Dysmyelination of auditory afferent axons increases the jitter of action potential timing during high-frequency firing. J. Neurosci. 33, 9402–9407. http://dx.doi.org/10.1523/JNEUROSCI.3389-12.2013.
Liebetanz, D., Merkler, D., 2006. Effects of commissural de- and remyelination on motor skill behaviour in the cuprizone mouse model of multiple sclerosis. Exp. Neurol. 202, 217–224. http://dx.doi.org/10.1016/j.expneurol.2006.05.032.
Long, P., Corfas, G., 2014. Dynamic regulation of myelination in health and disease. JAMA Psychiatry 71, 1296–1297. http://dx.doi.org/10.1001/jamapsychiatry.2014.1049.
Mandolesi, G., Grasselli, G., Musumeci, G., Centonze, D., 2010. Cognitive deficits in experimental autoimmune encephalomyelitis: neuroinflammation and synaptic degeneration. Neurol. Sci. 31, S255–S259. http://dx.doi.org/10.1007/s10072-010-0369-3.
Manrique-Hoyos, N., Jürgens, T., Grønborg, M., Kreutzfeldt, M., Schedensack, M., Kuhlmann, T., Schrick, C., Brück, W., Urlaub, H., Simons, M., Merkler, D., 2012. Late motor decline after accomplished remyelination: impact for progressive multiple sclerosis. Ann. Neurol. 71, 227–244. http://dx.doi.org/10.1002/ana.22681.
Markianos, M., Koutsis, G., Evangelopoulos, M.-E., Mandellos, D., Karahalios, G., Sfagos, C., 2009. Relationship of CSF neurotransmitter metabolite levels to disease severity and disability in multiple sclerosis. J. Neurochem. 108, 158–164. http://dx.doi.org/10.1111/j.1471-4159.2008.05750.x.
Markoullis, K., Sargiannidou, I., Schiza, N., Hadjisavvas, A., Roncaroli, F., Reynolds, R., Kleopa, K.A., 2012. Gap junction pathology in multiple sclerosis lesions and normal-appearing white matter. Acta Neuropathol. 123, 873–886. http://dx.doi.org/10.1007/s00401-012-0978-4.
Matas, C.G., Matas, S.L. de A., Oliveira, C.R.S. de, Gonçalves, I.C., 2010. Auditory evoked potentials and multiple sclerosis. Arq. Neuropsiquiatr. 68, 528–534.
Matsushima, G.K., Morell, P., 2001. The neurotoxicant, cuprizone, as a model to study demyelination and remyelination in the central nervous system. Brain Pathol. 11, 107–116.
McKenzie, I.A., Ohayon, D., Li, H., Paes de Faria, J., Emery, B., Tohyama, K., Richardson, W.D., 2014. Motor skill learning requires active central myelination. Science 346, 318–322. http://dx.doi.org/10.1126/science.1254960.
Meuth, S.G., Bittner, S., Ulzheimer, J.C., Kleinschnitz, C., Kieseier, B.C., Wiendl, H., 2010. Therapeutic approaches to multiple sclerosis: an update on failed, interrupted, or inconclusive trials of neuroprotective and alternative treatment strategies. BioDrugs 24, 317–330. http://dx.doi.org/10.2165/11537190-000000000-00000.
Minagar, A., Barnett, M.H., Benedict, R.H.B., Pelletier, D., Pirko, I., Sahraian, M.A., Frohman, E., Zivadinov, R., 2013. The thalamus and multiple sclerosis: Modern views on pathologic, imaging, and clinical aspects. Neurology 80, 210–219. http://dx.doi.org/10.1212/WNL.0b013e31827b910b.

Mullard, A., 2016. Remyelination researchers regroup after proof-of-concept setback in. Nat. Publ. Gr. 15, 519–521. http://dx.doi.org/10.1038/nrd.2016.158.
Musacchia, G., Large, E.W., Schroeder, C.E., 2014. Thalamocortical mechanisms for integrating musical tone and rhythm. Hear. Res. 308, 50–59. http://dx.doi.org/10.1016/j.heares.2013.09.017.
Muto, M., Mori, M., Sato, Y., Uzawa, A., Masuda, S., Uchida, T., Kuwabara, S., 2015. Current symptomatology in multiple sclerosis and neuromyelitis optica. Eur. J. Neurol. 22, 299–304. http://dx.doi.org/10.1111/ene.12566.
Narayanan, V., Heiming, R.S., Jansen, F., Lesting, J., Sachser, N., Pape, H.-C., Seidenbecher, T., 2011. Social defeat: impact on fear extinction and amygdala-prefrontal cortical theta synchrony in 5-HTT deficient mice. PLoS ONE 6, e22600. http://dx.doi.org/10.1371/journal.pone.0022600.
Nave, K.-A., Werner, H.B., 2014. Myelination of the nervous system: mechanisms and functions. Annu. Rev. Cell Dev. Biol. 30, 503–533. http://dx.doi.org/10.1146/annurev-cellbio-100913-013101.
Niklas, A., Sebraoui, H., Hess, E., Wagner, A., Then Bergh, F., 2009. Outcome measures for trials of remyelinating agents in multiple sclerosis: retrospective longitudinal analysis of visual evoked potential latency. Mult. Scler. 15, 68–74. http://dx.doi.org/10.1177/1352458508095731.
Parisi, L., Rocca, M.A., Mattioli, F., Riccitelli, G.C., Capra, R., Stampatori, C., Bellomi, F., Filippi, M., 2014. Patterns of regional gray matter and white matter atrophy in cortical multiple sclerosis. J. Neurol. 261, 1715–1725. http://dx.doi.org/10.1007/s00415-014-7409-5.
Pavelko, K.D., van Engelen, B.G., Rodriguez, M., 1998. Acceleration in the rate of CNS remyelination in lysolecithin-induced demyelination. J. Neurosci. 18, 2498–2505.
Paxinos, G., Franklin, K., 2001. The Mouse Brain in Stereotaxic Coordinates. Academic P. ed., London.
Pourabdolhossein, F., Mozafari, S., Morvan-Dubois, G., Mirnajafi-Zadeh, J., Lopez-Juarez, A., Pierre-Simons, J., Demeneix, B.A., Javan, M., 2014. Nogo receptor inhibition enhances functional recovery following lysolecithin-induced demyelination in mouse optic chiasm. PLoS ONE 9, e106378. http://dx.doi.org/10.1371/journal.pone.0106378.
Riccitelli, G., Rocca, M.A., Pagani, E., Rodegher, M.E., Rossi, P., Falini, A., Comi, G., Filippi, M., 2011. Cognitive impairment in multiple sclerosis is associated to different patterns of gray matter atrophy according to clinical phenotype. Hum. Brain Mapp. 32, 1535–1543. http://dx.doi.org/10.1002/hbm.21125.
Rodgers, J.M., Robinson, A.P., Miller, S.D., 2013. Strategies for protecting oligodendrocytes and enhancing remyelination in multiple sclerosis. Discov. Med. 16, 53–63.
Ruck, T., Bittner, S., Gross, C.C., Breuer, J., Albrecht, S., Korr, S., Göbel, K., Pankratz, S., Henschel, C.M., Schwab, N., Staszewski, O., Prinz, M., Kuhlmann, T., Meuth, S.G., Wiendl, H., 2013. CD4+NKG2D+ T cells exhibit enhanced migratory and encephalitogenic properties in neuroinflammation. PLoS ONE 8, e81455. http://dx.doi.org/10.1371/journal.pone.0081455.
Rudick, R.A., Mi, S., Sandrock, A.W., 2008. LINGO-1 antagonists as therapy for multiple sclerosis: in vitro and in vivo evidence. Expert Opin. Biol. Ther. 8, 1561–1570. http://dx.doi.org/10.1517/14712598.8.10.1561.
Sachs, H.H., Bercury, K.K., Popescu, D.C., Narayanan, S.P., Macklin, W.B., 2014. A new model of cuprizone-mediated demyelination/remyelination. ASN Neuro 6. http://dx.doi.org/10.1177/1759091414551955.
Sahin, N., Selouan, R., Markowitz, C.E., Melhem, E.R., Bilello, M., 2015. Limbic pathway lesions in patients with multiple sclerosis. Acta Radiol. http://dx.doi.org/10.1177/0284185115578689.
Sampaio-Baptista, C., Khrapitchev, A.A., Foxley, S., Schlagheck, T., Scholz, J., Jbabdi, S., DeLuca, G.C., Miller, K.L., Taylor, A., Thomas, N., Kleim, J., Sibson, N.R., Bannerman, D., Johansen-Berg, H., 2013. Motor skill learning induces changes in white matter microstructure and myelination. J. Neurosci. 33, 19499–19503. http://dx.doi.org/10.1523/JNEUROSCI.3048-13.2013.
Sanfilipo, M.P., Benedict, R.H.B., Weinstock-Guttman, B., Bakshi, R., 2006. Gray and white matter brain atrophy and neuropsychological impairment in multiple sclerosis. Neurology 66, 685–692. http://dx.doi.org/10.1212/01.wnl.0000201238.93586.d9.
Skripuletz, T., Gudi, V., Hackstette, D., Stangel, M., 2011. De- and remyelination in the CNS white and grey matter induced by cuprizone: the old, the new, and the unexpected. Histol. Histopathol. 26, 1585–1597.
Skripuletz, T., Hackstette, D., Bauer, K., Gudi, V., Pul, R., Voss, E., Berger, K., Kipp, M., Baumgärtner, W., Stangel, M., 2013. Astrocytes regulate myelin clearance through recruitment of microglia during cuprizone-induced demyelination. Brain 136, 147–167. http://dx.doi.org/10.1093/brain/aws262.
Skripuletz, T., Lindner, M., Kotsiari, A., Garde, N., Fokuhl, J., Linsmeier, F., Trebst, C., Stangel, M., 2008. Cortical demyelination is prominent in the murine cuprizone model and is strain-dependent. Am. J. Pathol. 172, 1053–1061. http://dx.doi.org/10.2353/ajpath.2008.070850.
Sutor, B., Schmolke, C., Teubner, B., Schirmer, C., Willecke, K., 2000. Myelination defects and neuronal hyperexcitability in the neocortex of connexin 32-deficient mice. Cereb. Cortex 10, 684–697. http://dx.doi.org/10.1093/cercor/10.7.684.
Tewarie, P., Hillebrand, A., Schoonheim, M.M., van Dijk, B.W., Geurts, J.J., Barkhof, F., Polman, C., Stam, C.J., 2014a. Functional brain network analysis using minimum spanning trees in multiple sclerosis: an MEG source-space study. Neuroimage 88, 308–318. http://dx.doi.org/10.1016/j.neuroimage.2013.10.022.
Tewarie, P., Steenwijk, M.D., Tijms, B.M., Daams, M., Balk, L.J., Stam, C.J., Uitdehaag, B.M.J., Polman, C.H., Geurts, J.J.G., Barkhof, F., Pouwels, P.J.W., Vrenken, H., Hillebrand, A., 2014b. Disruption of structural and functional networks in long-standing multiple sclerosis. Hum. Brain Mapp. 35, 5946–5961. http://dx.doi.org/10.1002/hbm.22596.
Vercellino, M., Plano, F., Votta, B., Mutani, R., Giordana, M.T., Cavalla, P., 2005. Grey matter pathology in multiple sclerosis. J. Neuropathol. Exp. Neurol. 64, 1101–1107. http://dx.doi.org/10.1097/01.jnen.0000190067.20935.42.
Villain, N., Fouquet, M., Baron, J.-C., Mézenge, F., Landeau, B., de La Sayette, V., Viader, F., Eustache, F., Desgranges, B., Chételat, G., 2010. Sequential relationships between grey matter and white matter atrophy and brain metabolic abnormalities in early Alzheimer's disease. Brain 133, 3301–3314. http://dx.doi.org/10.1093/brain/awq203.
Xu, H., Yang, H.-J., Zhang, Y., Clough, R., Browning, R., Li, X.-M., 2009. Behavioral and neurobiological changes in C57BL/6 mice exposed to cuprizone. Behav. Neurosci. 123, 418–429. http://dx.doi.org/10.1037/a0014477.
Yates, D., 2014. Myelination: switching modes of myelination. Nat. Rev. Neurosci. 15, 66–67. http://dx.doi.org/10.1038/nrn3682.
Yeung, M.S.Y., Zdunek, S., Bergmann, O., Bernard, S., Salehpour, M., Alkass, K., Perl, S., Tisdale, J., Possnert, G., Brundin, L., Druid, H., Frisén, J., 2014. Dynamics of oligodendrocyte generation and myelination in the human brain. Cell 159, 766–774. http://dx.doi.org/10.1016/j.cell.2014.10.011.
Zarei, M., Chandran, S., Compston, A., Hodges, J., 2003. Cognitive presentation of multiple sclerosis: evidence for a cortical variant. J. Neurol. Neurosurg. Psychiatry 74, 872–877.
Zhang, H., Zhang, Y., Xu, H., Wang, L., Zhao, J., Wang, J., Zhang, Z., Tan, Q., Kong, J., Huang, Q., Li, X.-M., 2013. Locomotor activity and anxiety status, but not spatial working memory, are affected in mice after brief exposure to cuprizone. Neurosci. Bull. 29, 633–641. http://dx.doi.org/10.1007/s12264-013-1369-0.
Zhou, J., Zhuang, J., Li, J., Ooi, E., Bloom, J., Poon, C., Lax, D., Rosenbaum, D.M., Barone, F.C., 2013. Long-term post-stroke changes include myelin loss, specific deficits in sensory and motor behaviors and complex cognitive impairment detected using active place avoidance. PLoS ONE 8, e57503. http://dx.doi.org/10.1371/journal.pone.0057503.